Supplementary Information

Chain-Stiffening Enhanced Ultralong Organic Phosphorescence in High Glass Transition Temperature Polymers

Huan Chen,[a†] Mengyang Dong,[*a†] Yanxin Wu,[a] Jingyi Shan,[a] Zehua Long,[a] Yaru Gao[*b] and Long Gu[*a]

[a] State Key Laboratory of Flexible Electronics (LOFE) & Institute of Flexible Electronics (IFE), Ningbo Institute of Northwestern Polytechnical University, Northwestern Polytechnical University, 127 West Youyi Road, Xi'an, 710072, China
[b] School of Chemistry, Chemical Engineering and Biotechnology, Nanyang Technological University, Singapore 637371, Singapore

[†]These authors contributed equally to this work

*Correspondence to: dongmengyang@mail.nwpu.edu.cn; yaru.gao@ntu.edu.sg; iamlgu@nwpu.edu.cn

Measurements

Nuclear magnetic resonance (^{1}H NMR and ^{13}C NMR) spectra were obtained on Bruker Ultra Shield Plus 500 MHz spectrometer. The chemical shift was relative to tetramethylsilane (TMS) as the internal standard. Resonance patterns were reported with the notation s (singlet), d(doublet), t (triplet), q (quartet), and m (multiplet). Gel permeation chromatography (GPC) measurements were performed on an Agilent 1260 HPLC system equipped with a G7110B pump and a G7162A refractive index detector, tetrahydrofuran was used as the eluent at 0.5 mL min^{-1} flow rate and PMMA was used as the standard. Steady-state fluorescence and phosphorescence spectra and lifetimes were measured using a fluorescence spectrophotometer (Edinburgh FLS1000) equipped with a xenon arc lamp, a nanosecond hydrogen flash-lamp, or a microsecond flash-lamp, and all the phosphorescence spectra were recorded with a delay time of 8 ms. DSC experiments were carried out under N_2 atmosphere using a NETZSCH DSC 214 system at a scan rate of 10 °C /min^{-1}. The thermal stability property was evaluated by thermogravimetric analysis (TGA) with the thermal analysis instrument (NETZSCH TG 209 F3) over the temperature range of 25-500 °C in an N_2 atmosphere with a heating rate of 10 °C/min^{-1} (empty Al_2O_3 crucible as the reference). Luminescent photographs were taken by a Canon EOS 850D camera.

Computational details:

The Time-Dependent Density Functional Theory (TD-DFT) approach[1] was used to investigate the excitation energies and spin-orbit coupling matrix elements (SOCMEs) of the singlet and triplet states of the RTP chromophores. The optimized geometries were carried out at M06-2X/def2-SVP level. The above results were performed by Gaussian 09 package.[2] At the same level, SOCMEs were evaluated through ORCA software.[3]

General procedure for the synthesis of monomers, copolymers, and chromophores.

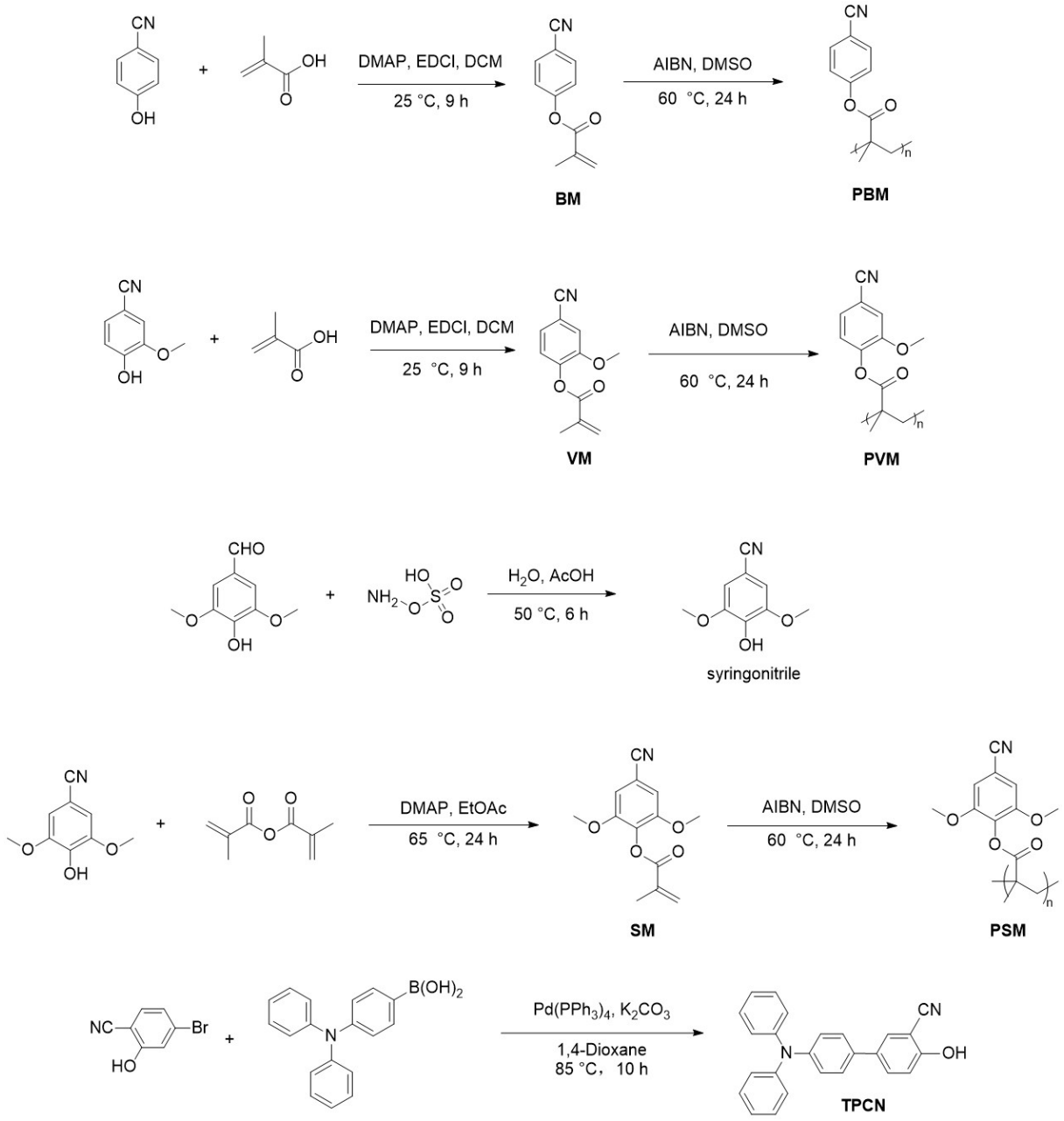

Fig. S1 | Synthetic routes of the target monomers (BM, VM, and SM), copolymers (PBM, PVM, and PSM), and chromophore (TPCN).

Synthetic procedures:

Compound BM:

4-hydroxybenzonitrile (1.00 g, 8.39 mmol), 4-Dimethylaminopyridine (DMAP, 2.05 g, 16.79 mmol), and 1-(3-Dimethylaminopropyl)-3-ethylcarbodiimide hydrochloride (EDCl, 3.22 g, 16.79 mmol) were dissolved in 25 mL of dichloromethane. Methyl methacrylate (0.73 g, 8.48 mmol) was added dropwise to the reaction mixture under a nitrogen atmosphere. After stirring the mixture solution at room temperature for 9 hours, the

solvent was removed using rotary evaporation. The residue was then purified by column chromatography, yielding BM as a white solid (1.32 g, 84%). ^{1}H NMR (500 MHz, DMSO-d_6) δ 7.98-7.92 (m, 2H), 7.48-7.41 (m, 2H), 6.32 (t, J = 1.2 Hz, 1H), 5.96 (q, J = 1.6 Hz, 1H), 2.01 (t, J = 1.3 Hz, 3H). ^{13}C NMR (126 MHz, $CDCl_3$) δ 163.89, 153.22, 134.23, 132.65, 127.35, 121.79, 117.26, 108.67, 17.26.

Polymer PBM:

The polymer was synthesized by radical copolymerization. BM (1.00 g, 5.34 mmol) and azobisisobutyronitrile (AIBN, 0.0088 g, 0.053 mmol) were dissolved in dimethyl sulfoxide (DMSO) of 10 mL under a nitrogen atmosphere. After stirring the solution at 60 °C for 24 h, the mixture was cooled to room temperature, and the white solids were obtained by precipitation in water. The crude product was then collected by filtration and washed repeatedly with water. Finally, the final product was obtained after vacuum drying at 50 °C.

Compound VM:

Vanillin cyanohydrin (1.00 g, 6.70 mmol), DMAP (1.64 g, 13.41 mmol), and EDCl (2.57 g, 13.41 mmol) were dissolved in 25 mL of dichloromethane. Methyl methacrylate (0.58 g, 6.77 mmol) was added dropwise to the reaction mixture under a nitrogen atmosphere. After stirring the mixture solution at room temperature for 9 hours, the solvent was removed using rotary evaporation. The residue was then purified by column chromatography, yielding VM as a white solid (1.23 g, 84%). ^{1}H NMR (500 MHz, DMSO-d_6) δ 7.68 (d, J = 1.9 Hz, 1H), 7.50 (dd, J = 8.1, 1.8 Hz, 1H), 7.38 (d, J = 8.2 Hz, 1H), 6.29 (t, J = 1.2 Hz, 1H), 5.94 (t, J = 1.6 Hz, 1H), 3.84 (s, 3H), 1.99 (t, J = 1.2 Hz, 3H). ^{13}C NMR (126 MHz, $CDCl_3$) δ 164.54, 153.09, 135.07, 133.16, 128.18, 118.76, 109.94, 109.10, 56.66, 18.56.

Polymer PVM:

VM (1 g, 4.60 mmol) and AIBN (0.0076 g, 0.046 mmol) were dissolved in 10 mL of dimethyl sulfoxide (DMSO) under a nitrogen atmosphere. After stirring the solution at 60 °C for 24 h, the mixture was cooled to room temperature, and the white solids were obtained by precipitation in water. The crude product was then collected by filtration and washed repeatedly with water. Finally, the final product was obtained after vacuum drying at 50 °C.

Compound syringonitrile:

4-hydroxy-3,5-dimethoxybenzaldehyde (2.00 g, 10.98 mmol) and hydroxylamine-O-sulfonic acid (1.366 g, 12.08 mmol) were dissolved in a mixture of water (20 mL) and acetic acid (20 mL) at 0 °C. The reaction mixture was stirred at 50 °C for 6 h, then quenched with 10% $NaHCO_3$ solution. After removing the solvent,

the crude product was purified by recrystallization from hexane, yielding syringonitrile as a light brown powder (1.62 g, 82%).

Compound SM:

4-hydroxy-3,5-dimethoxybenzonitrile (1.00 g, 5.58 mmol) and DMAP (13.44 mg, 0.11 mmol) were dissolved in 25 mL ethyl acetate. Methyl methacrylate (0.87 g, 5.64 mmol) was added dropwise to the reaction mixture under a nitrogen atmosphere. After stirring the mixture solution at 65 °C for 24 h, the solvent was removed using rotary evaporation. The residue was then purified by column chromatography, yielding SM as a white solid (1.08 g, 78%). ^{1}H NMR (500 MHz, Chloroform-*d*) δ 6.90 (s, 2H), 6.38 (t, *J* = 1.2 Hz, 1H), 5.79 (p, *J* = 1.5 Hz, 1H), 3.84 (s, 6H), 2.07 (t, *J* = 1.3 Hz, 3H). ^{13}C NMR (126 MHz, $CDCl_3$) δ 164.54, 153.09, 135.07, 133.16, 128.18, 118.76, 109.94, 109.10, 56.66, 18.56.

Polymer PSM:

SM (1.00 g, 4.04 mmol) and AIBN (0.00657 g, 0.040 mmol) were dissolved in dimethyl sulfoxide (DMSO) of 10 mL under a nitrogen atmosphere. After stirring the solution at 60 °C for 24 h, the mixture was cooled to room temperature, and the white solids were obtained by precipitation in water. The crude product was then collected by filtration and washed repeatedly with water. Finally, the final product was obtained after vacuum drying at 50 °C.

Compound TPCN (4'-(diphenylamino)-4-hydroxy-[1,1'-biphenyl]-3-carbonitrile):

4-boronotriphenylamine (1.00 g, 3.46 mmol), 4-bromo-2-hydroxybenzonitrile (0.82 g, 4.15 mmol), and 4, 3-phenylphosphine palladium (0.2 g, 0.173 mmol) were added to a 150 mL round-bottom flask. Under a nitrogen atmosphere, a degassed solution of anhydrous K_2CO_3 (1.43 g, 10.38 mmol) in 1,4-dioxane (50 mL) was then added to the reaction mixture. After stirring the mixture solution at 85 °C for 10 h, the solvent was removed by rotary evaporation. The residue was purified by column chromatography (Chloroform/*n*-hexane) to afford TPCN as a green powder (1.10 g, 88%). ^{1}H NMR (500 MHz, DMSO-d_6) δ 11.16 (s, 1H), 7.66 – 7.61 (m, 1H), 7.58 – 7.54 (m, 2H), 7.37 – 7.33 (m, 4H), 7.21 – 7.18 (m, 2H), 7.09 (td, J = 8.3, 1.2 Hz, 6H), 7.05 – 7.00 (m, 2H). ^{13}C NMR (126 MHz, $CDCl_3$) δ 136.19, 129.99, 129.25, 129.20, 126.88, 125.48, 125.22, 123.32, 117.76, 112.61.

Compound DBCz (7H-dibenzo[c,g]carbazole):

The reagents were purchased from commercial sources and further purified by column chromatography. ^{1}H NMR (500 MHz, Chloroform-*d*) δ 9.23 (d, *J* = 8.4 Hz, 2H), 8.75 (s, 1H), 8.05 (dd, *J* = 8.1, 1.4 Hz, 2H), 7.88 (d, *J* = 8.7 Hz, 2H), 7.72-7.67 (m, 4H), 7.53 (ddd, *J* = 7.9, 6.8, 1.1 Hz, 2H). ^{13}C NMR (126 MHz, $CDCl_3$)

δ 136.19, 129.99, 129.25, 129.20, 126.88, 125.48, 125.22, 123.32, 117.76, 112.61.

Compound Cone (Coronene):

The reagents were purchased from commercial sources and further purified by column chromatography.

^{1}H NMR (500 MHz, Chloroform-*d*) δ 8.83 (s, 12H). ^{13}C NMR (126 MHz, $CDCl_3$) δ 127.72, 125.16, 121.58.

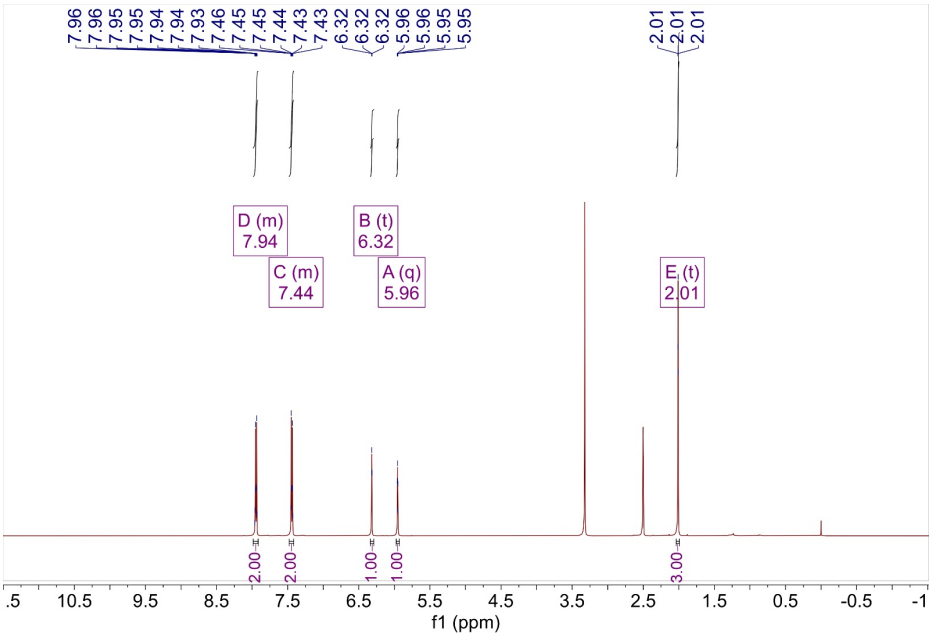

Fig. S2 | ^{1}H NMR spectrum of the BM molecule in DMSO-*d*$_6$ under ambient conditions.

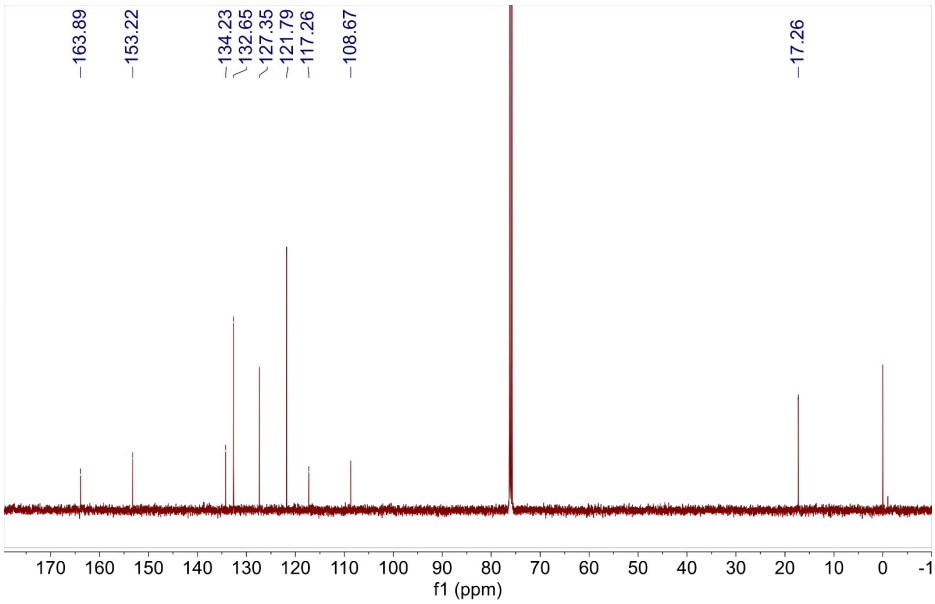

Fig. S3 | ^{13}C NMR spectrum of the BM molecule in $CDCl_3$ under ambient conditions.

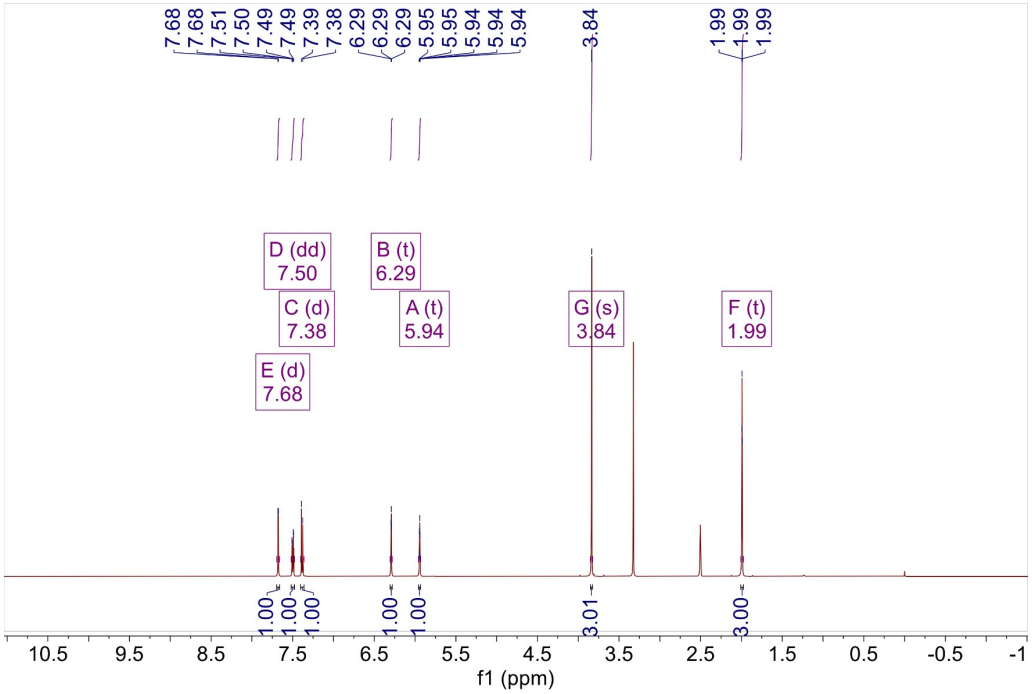

Fig. S4 | ^{1}H NMR spectrum of the VM molecule in DMSO-d_6 under ambient conditions.

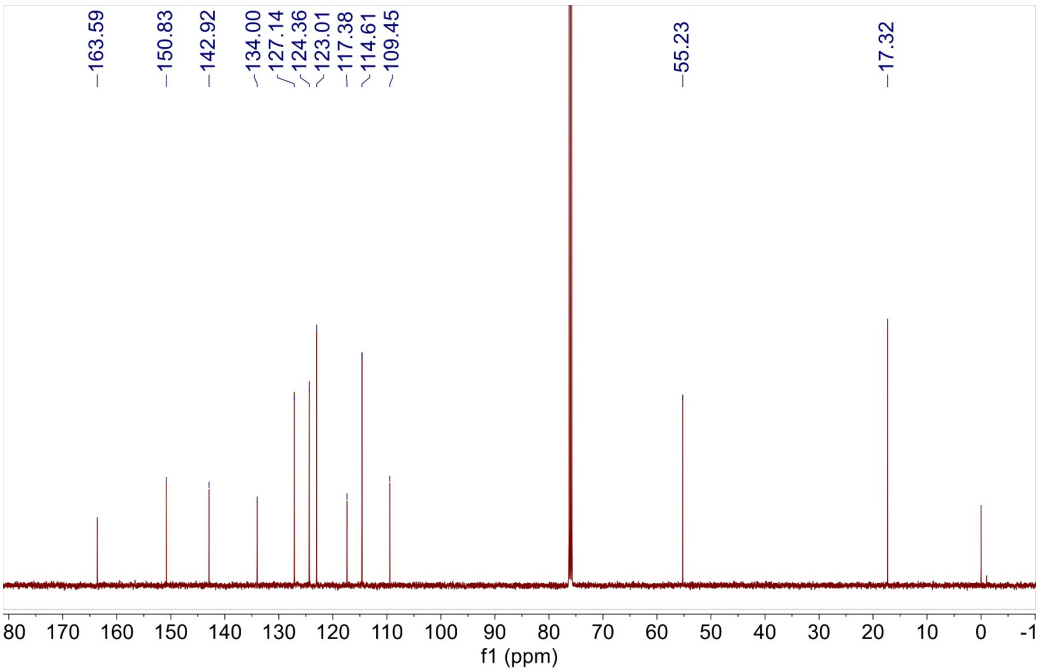

Fig. S5 | ^{13}C NMR spectrum of the VM molecule in $CDCl_3$ under ambient conditions.

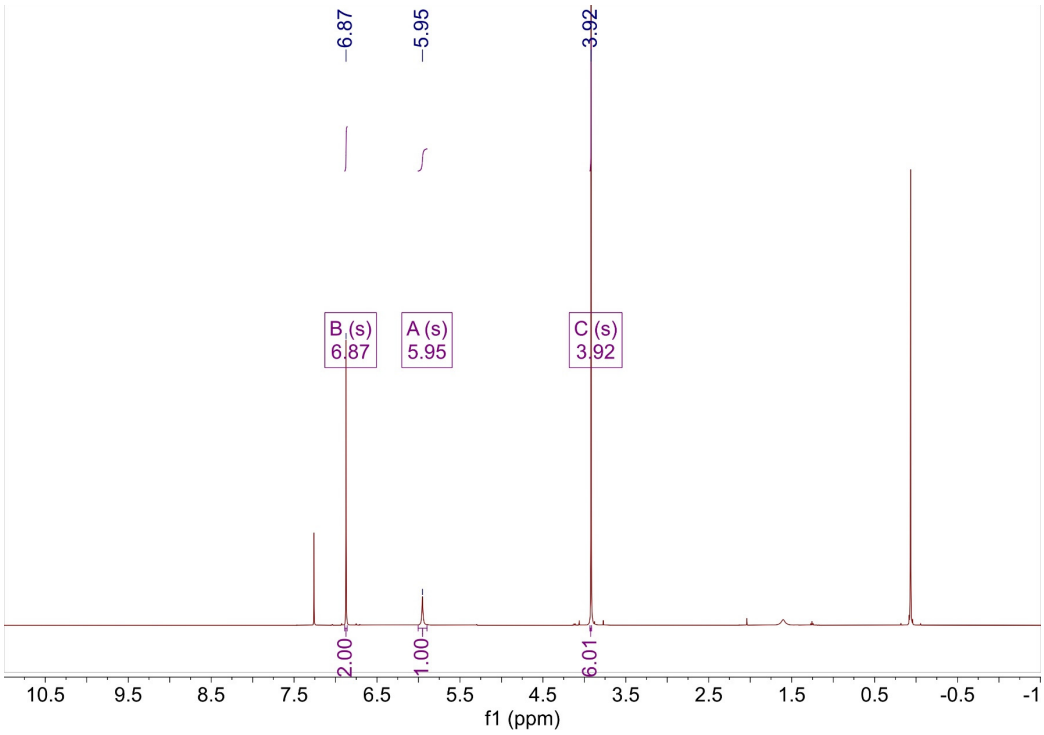

Fig. S6 | ^{1}H NMR spectrum of the syringonitrile molecule in $CDCl_3$ under ambient conditions.

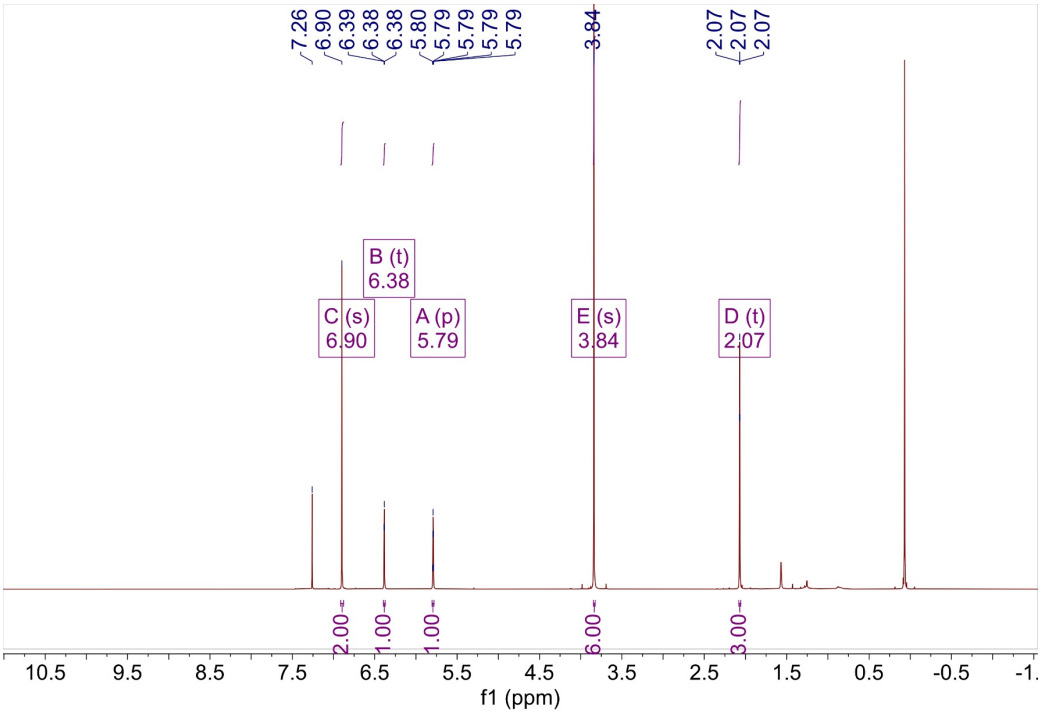

Fig. S7 | ^{1}H NMR spectrum of the SM molecule in $CDCl_3$ under ambient conditions.

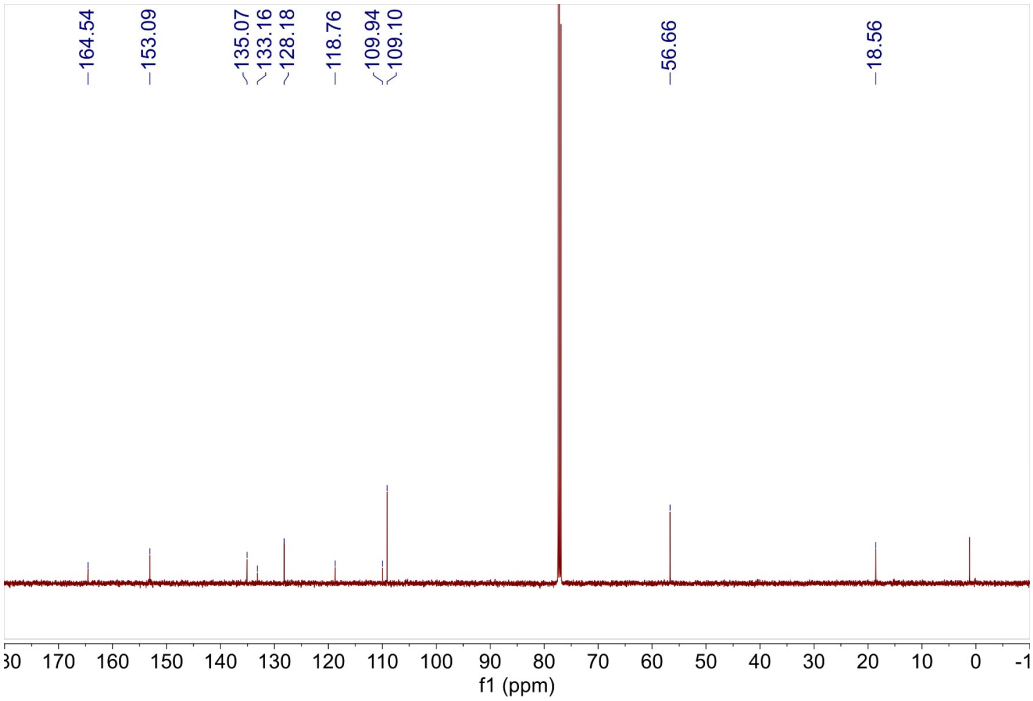

Fig. S8 | ^{13}C NMR spectrum of the SM molecule in $CDCl_3$ under ambient conditions.

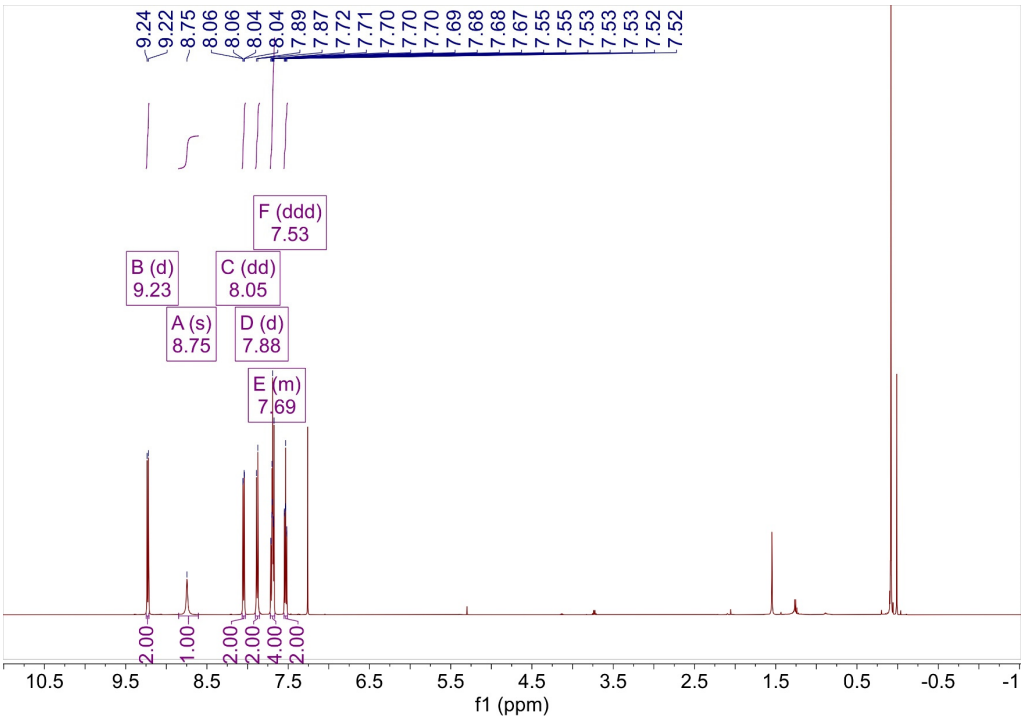

Fig. S9 | ^{1}H NMR spectrum of the DBCz molecule in $CDCl_3$ under ambient conditions.

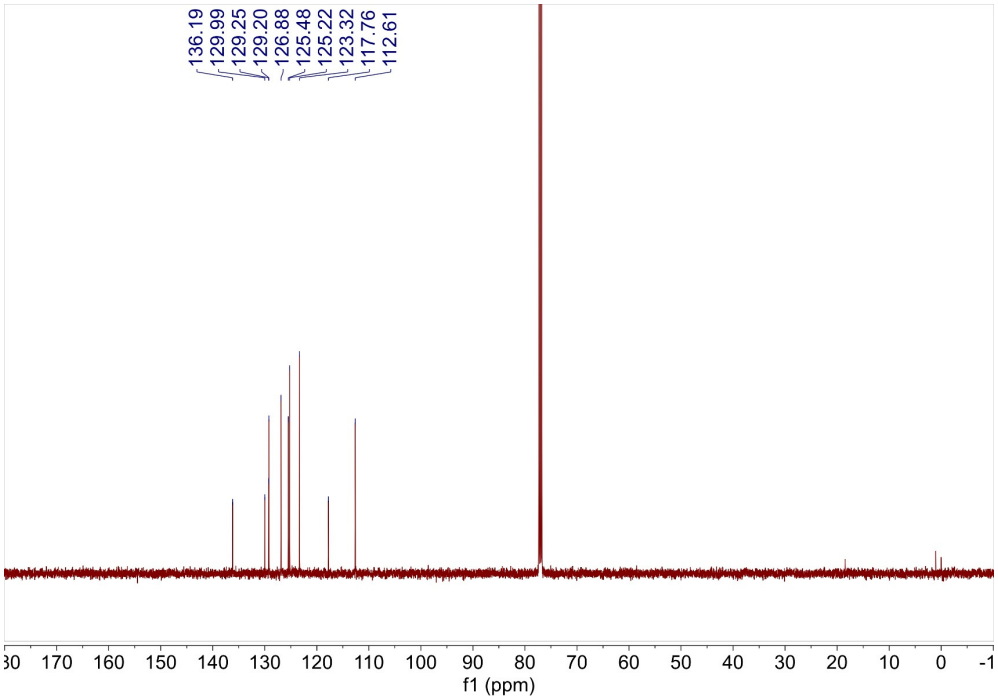

Fig. S10 | ^{13}C NMR spectrum of DBCz molecule in $CDCl_3$ under ambient conditions.

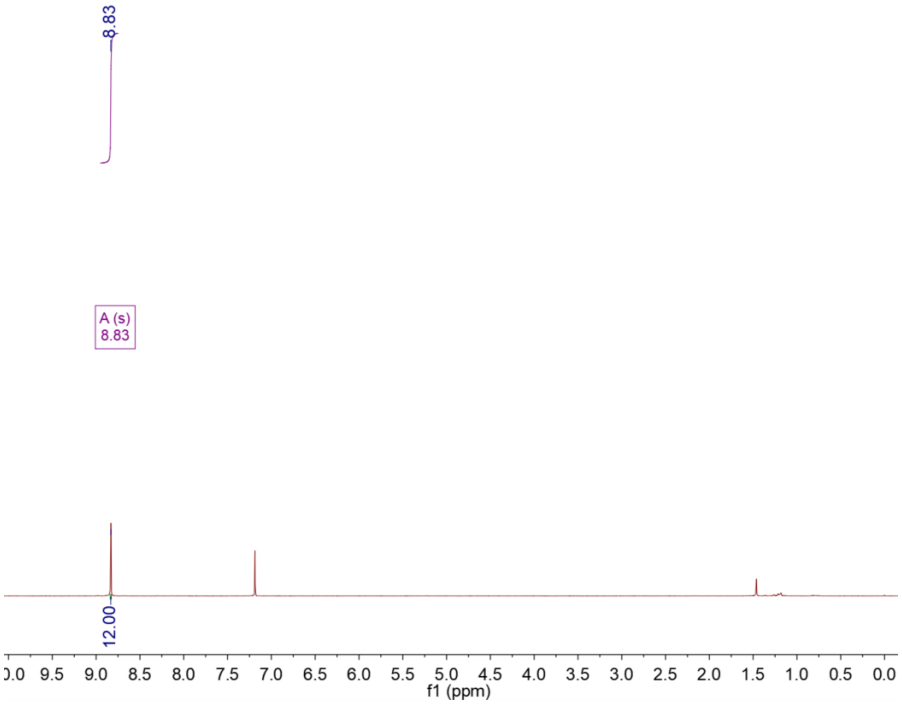

Fig. S11 | ^{1}H NMR spectrum of the Cone molecule in $CDCl_3$ under ambient conditions.

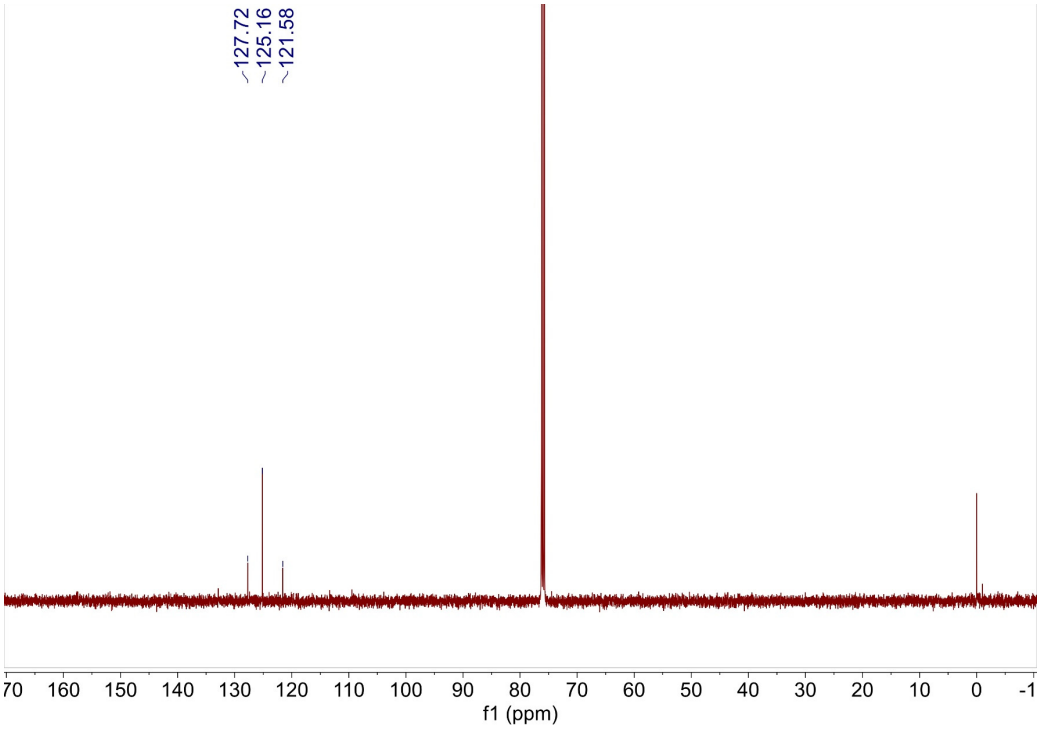

Fig. S12 | ^{13}C NMR spectrum of the Cone molecule in $CDCl_3$ under ambient conditions.

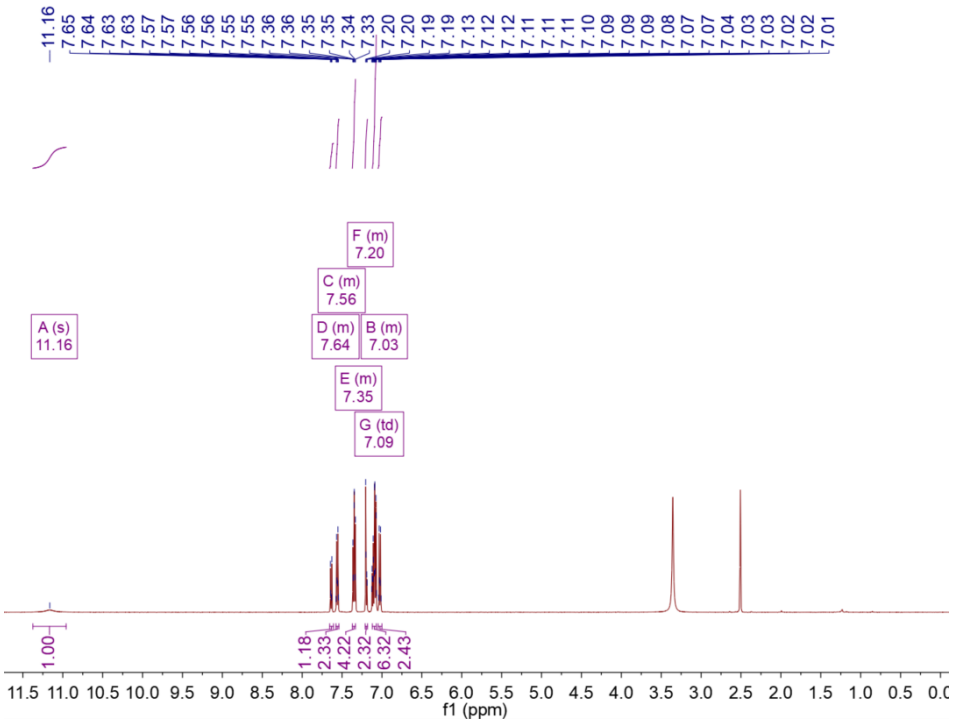

Fig. S13 | ^{1}H NMR spectrum of the TPCN molecule in DMSO-d_6 under ambient conditions.

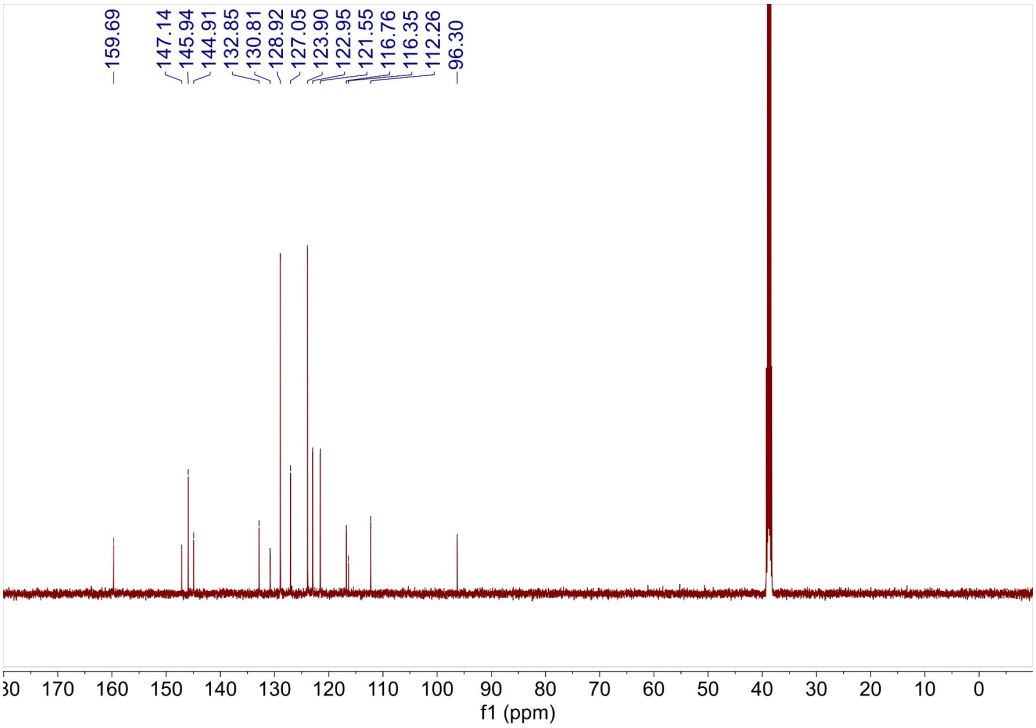

Fig. S14 | ^{13}C NMR spectrum of the TPCN molecule in DMSO-d_6 under ambient conditions.

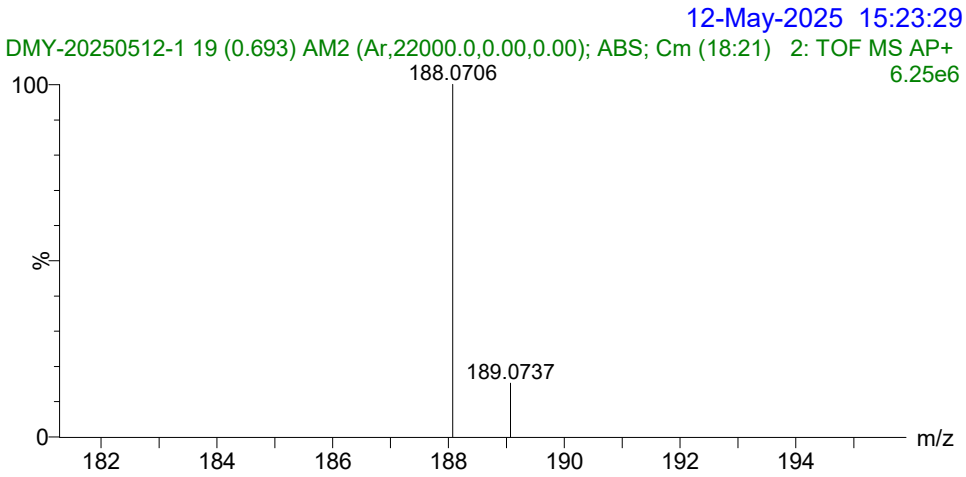

Fig. S15 | HR mass spectrum of BM in acetonitrile. $(BM+H)^+$ m/z: 188.0706 (theoretical value: 188.0706).

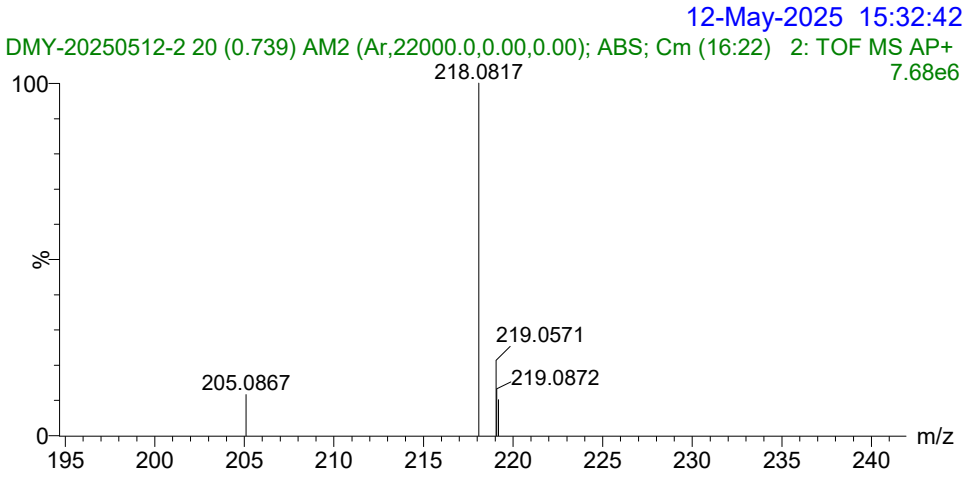

Fig. S16 | HR mass spectrum of VM in acetonitrile. $(VM+H)^+$ m/z: 218.0817 (theoretical value: 218.0812).

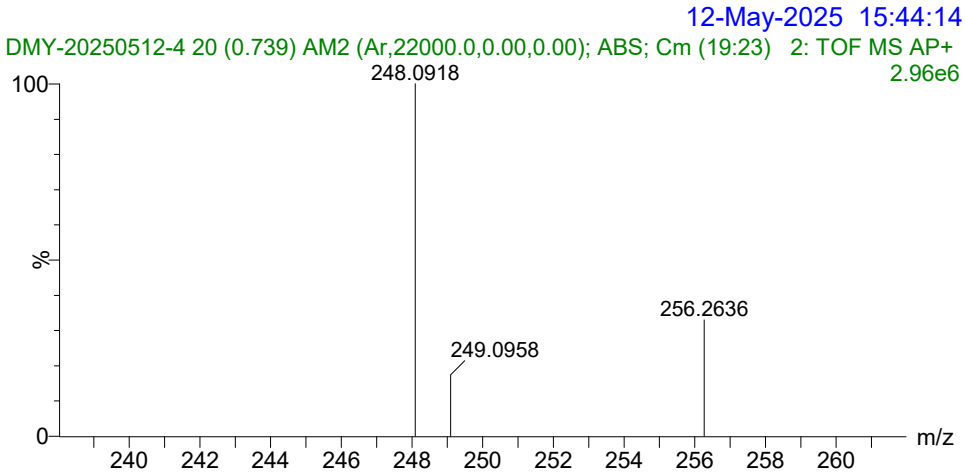

Fig. S17 | HR mass spectrum of SM in acetonitrile. $(SM+H)^+$ m/z: 248.0918 (theoretical value: 248.0918).

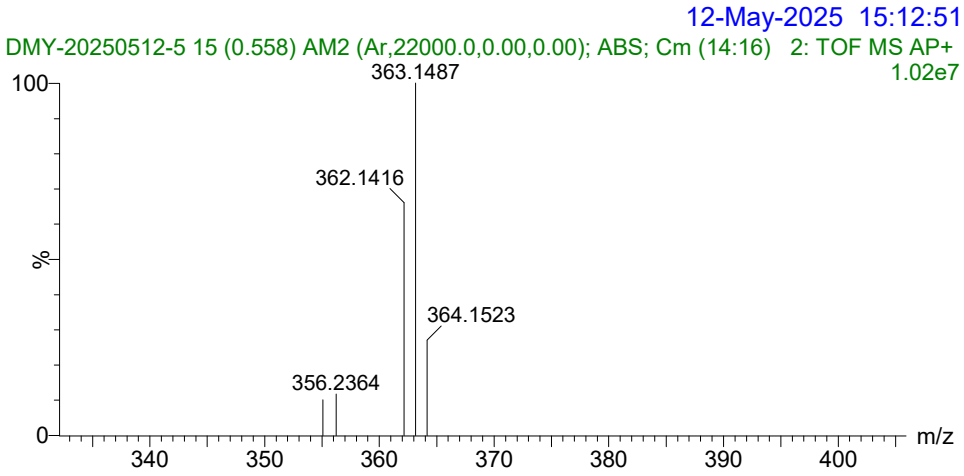

Fig. S18 | HR mass spectrum of TPCN in acetonitrile. (TPCN) m/z: 362.1416 (theoretical value: 362.1419).

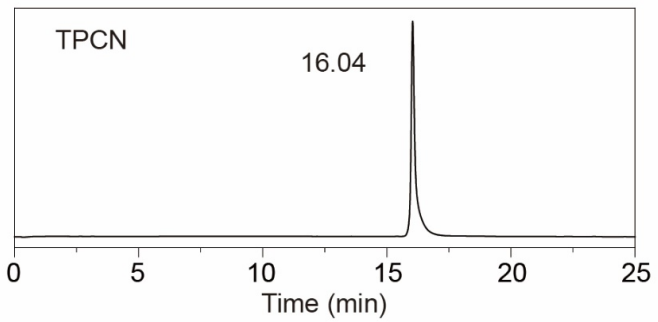

Fig. S19 | High-performance liquid chromatograph spectrum of TPCN in acetonitrile (mobile phase: 70% acetonitrile/ 30% water).

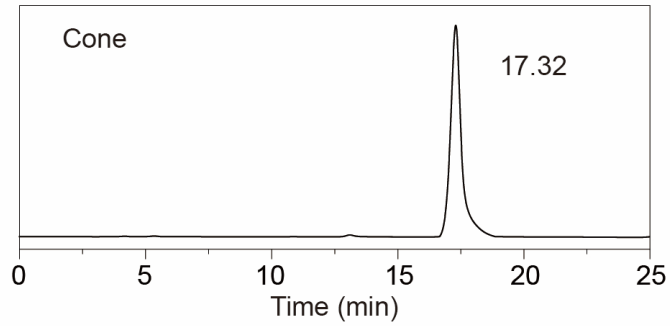

Fig. S20 | High-performance liquid chromatograph spectrum of Cone in acetonitrile (mobile phase: 90% acetonitrile/10% water).

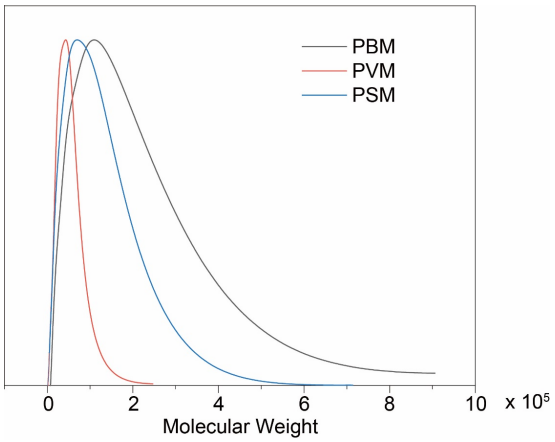

Fig. S21 | Gel permeation chromatography characterization of copolymers PBM, PVM, and PSM.

Table S1. Characterizations of copolymers PBM, PVM, and PSM.

Sample	**PBM**	**PVM**	**PSM**
M_n	53362	20889	27861
PDI	2.61	1.85	2.78

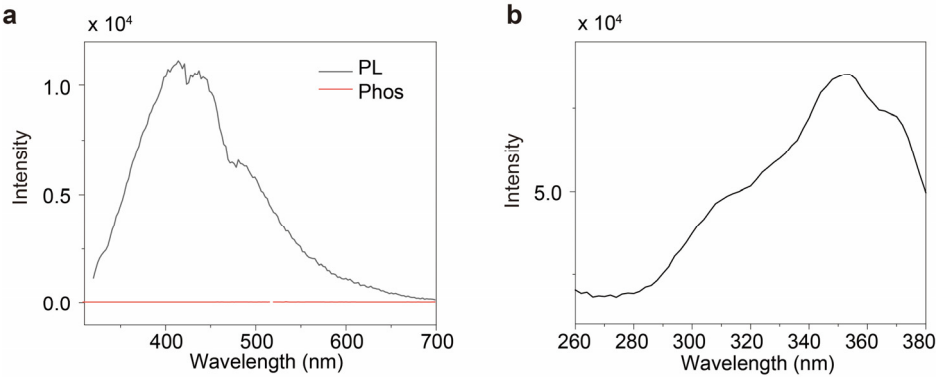

Fig. S22 | (a) Photoluminescence (PL) and phosphorescence (Phos.) spectra of PBM polymers under ambient conditions. (b) Photoluminescence excitation spectra of PBM polymers at 406 nm under ambient condition.

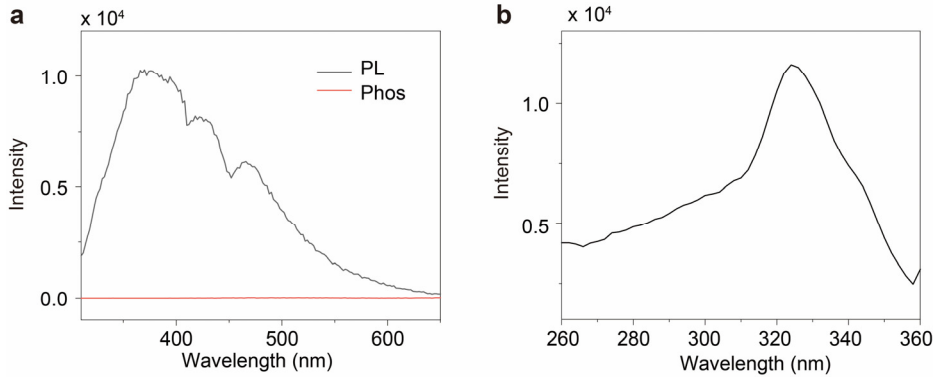

Fig. S23 | (a) Photoluminescence (PL) and phosphorescence (Phos.) spectra of PVM polymers under ambient conditions. (b) Photoluminescence excitation spectra of PBM polymers at 376 nm under ambient condition.

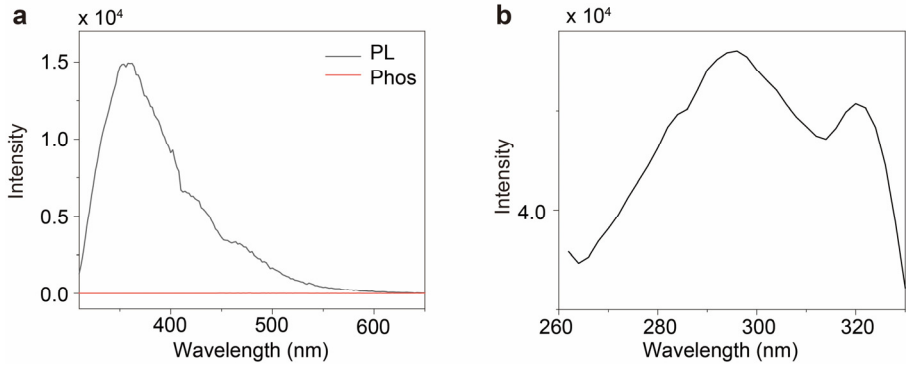

Fig. S24 | (a) Photoluminescence (PL) and phosphorescence (Phos.) spectra of PVM polymers under ambient conditions. (b) Photoluminescence excitation spectra of PBM polymers at 354 nm under ambient condition.

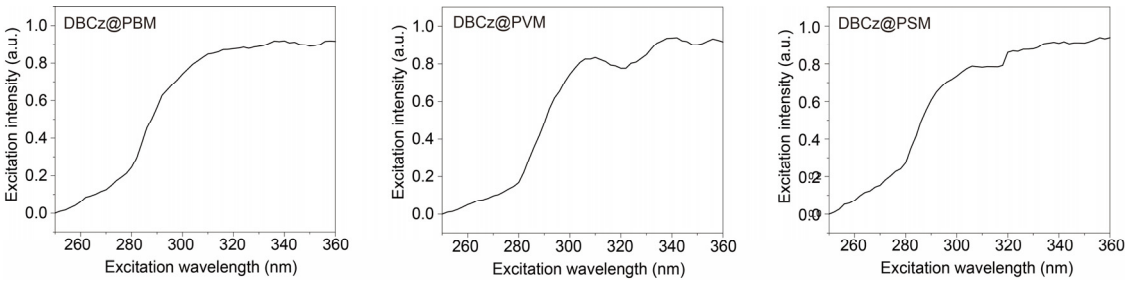

Fig. S25 | Normalized photoluminescence excitation spectra of DBCz@PBM, DBCz@PVM and DBCz@PSM at 395 nm under ambient conditions.

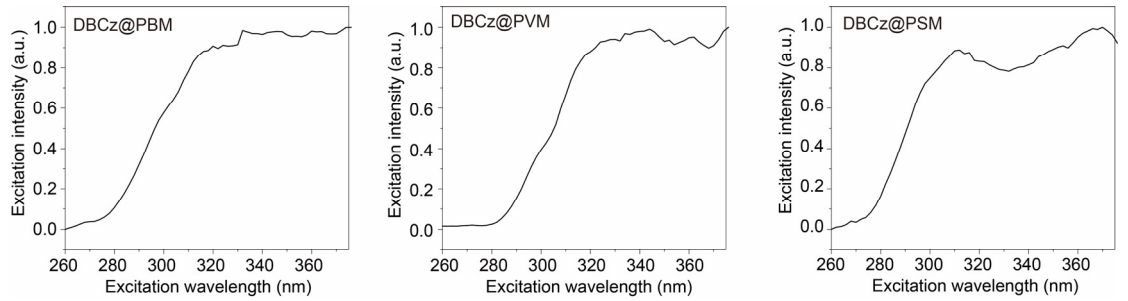

Fig. S26 | Normalized phosphorescence excitation spectra of DBCz@PBM, DBCz@PVM and DBCz@PSM at 520 nm under ambient conditions.

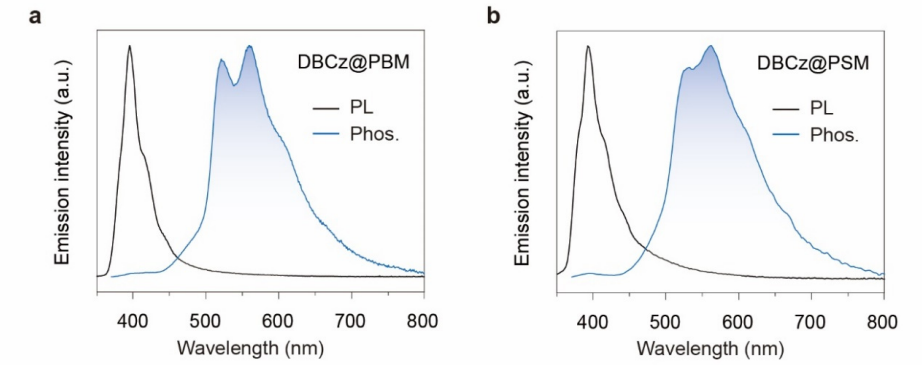

Fig. S27 | Normalized steady-state photoluminescence (black lines) and phosphorescence (blue lines) spectra of a) DBCz@PBM, and b) DBCz@PSM films.

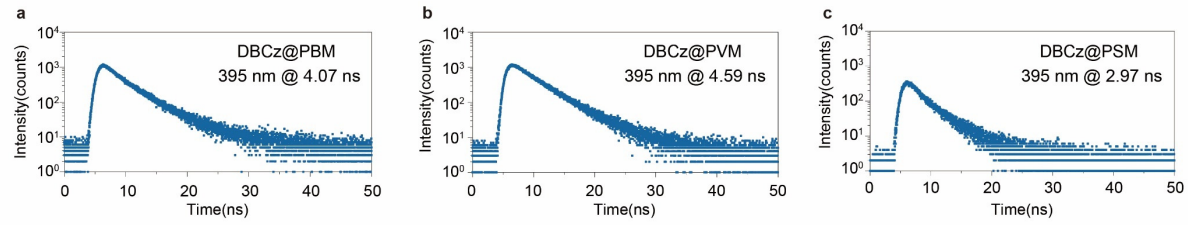

Fig. S28 | Fluorescence lifetime decay curves of a) DBCz@PBM, b) DBCz@PVM and c) DBCz@PSM films under ambient conditions.

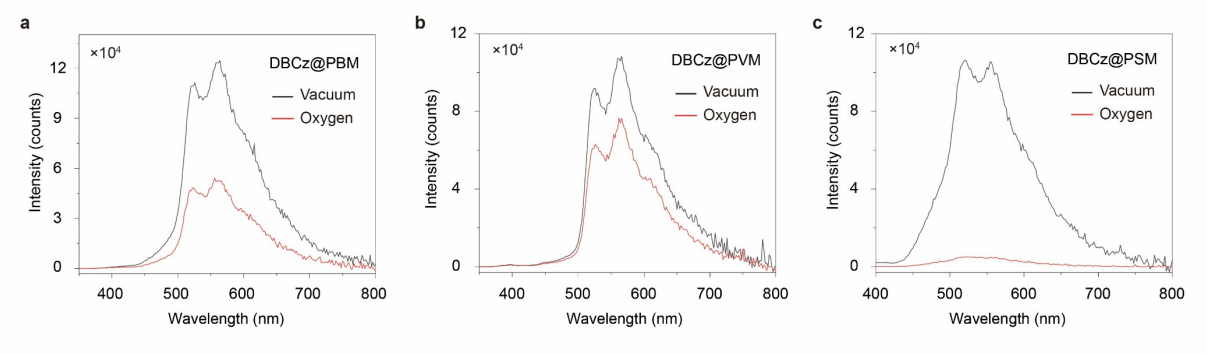

Fig. S29 | Phosphorescence spectra of a) DBCz@PBM, b) DBCz@PVM, and c) DBCz@PSM film in vacuum (black lines) and after exposure to oxygen (red lines) for 10 min.

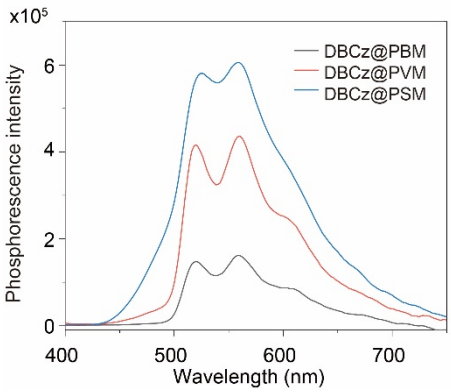

Fig. S30 | Phosphorescence intensity of DBCz@PBM, DBCz@PVM and DBCz@PSM under vacuum conditions at room temperature.

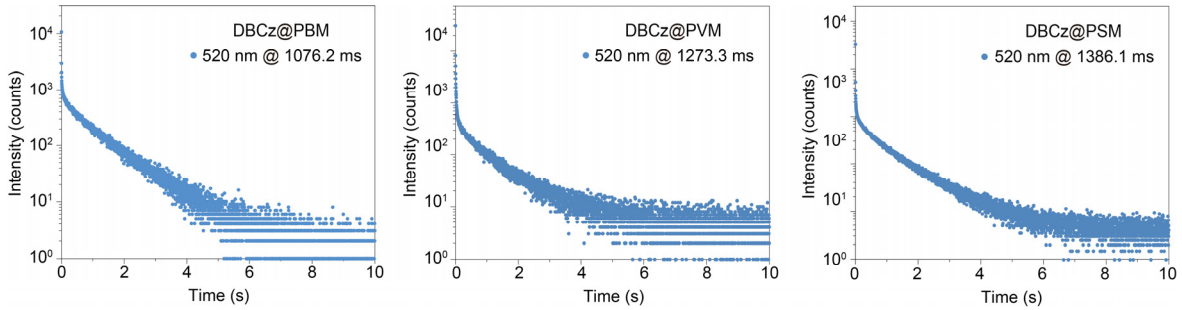

Fig. S31 | Phosphorescence lifetime of DBCz@PBM, DBCz@PVM and DBCz@PSM under vacuum conditions at room temperature.

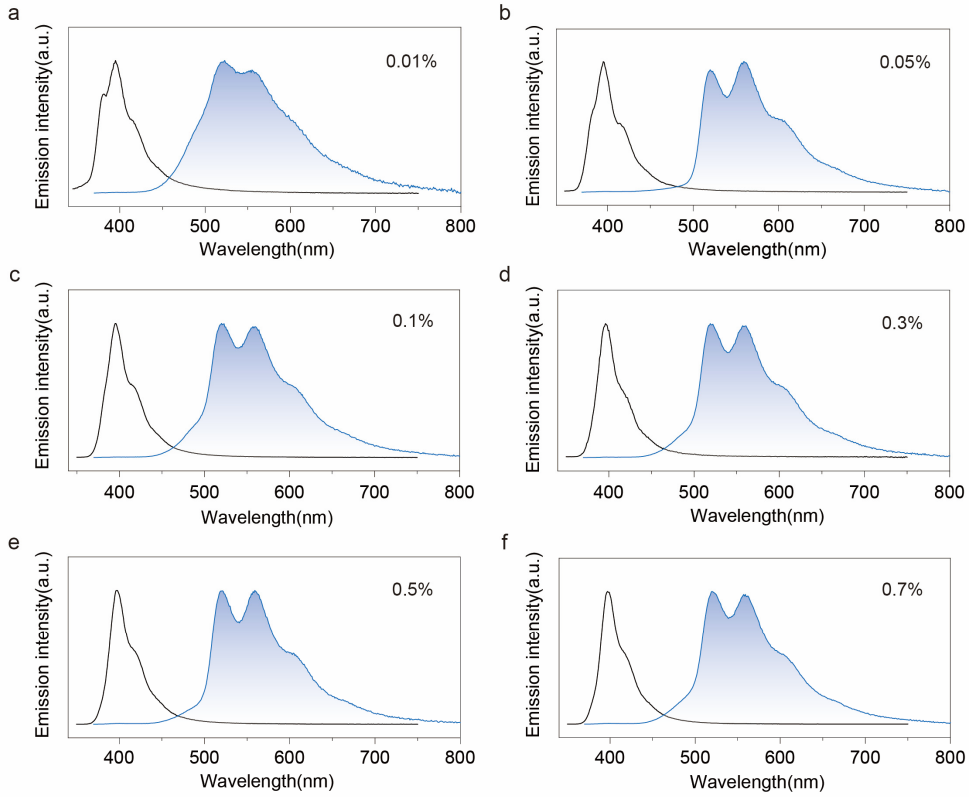

Fig. S32 | Normalized steady-state photoluminescence (black lines) and phosphorescence (blue lines) spectra of DBCz in PVM films. a, 0.01 wt.%. b, 0.05 wt.%. c, 0.1 wt.%. d, 0.3 wt.%. e, 0.5 wt.%. f, 0.7 wt.%.

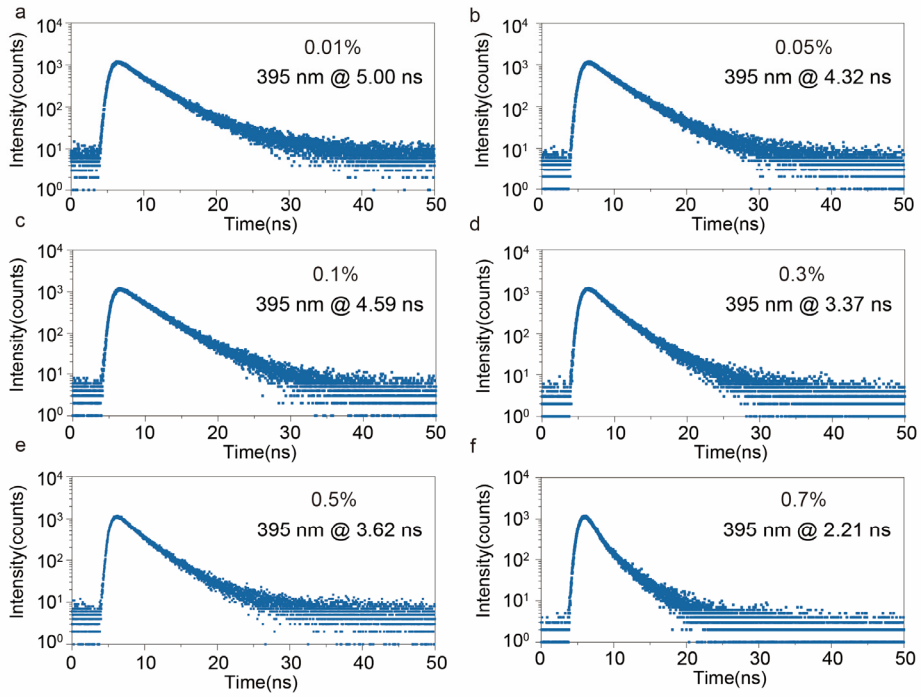

Fig. S33 | Fluorescence lifetime of DBCz@PVM films under ambient conditions. a, 0.01 wt.%. b, 0.05 wt.%. c, 0.1 wt.%. d, 0.3 wt.%. e, 0.5 wt.%. f, 0.7 wt.%.

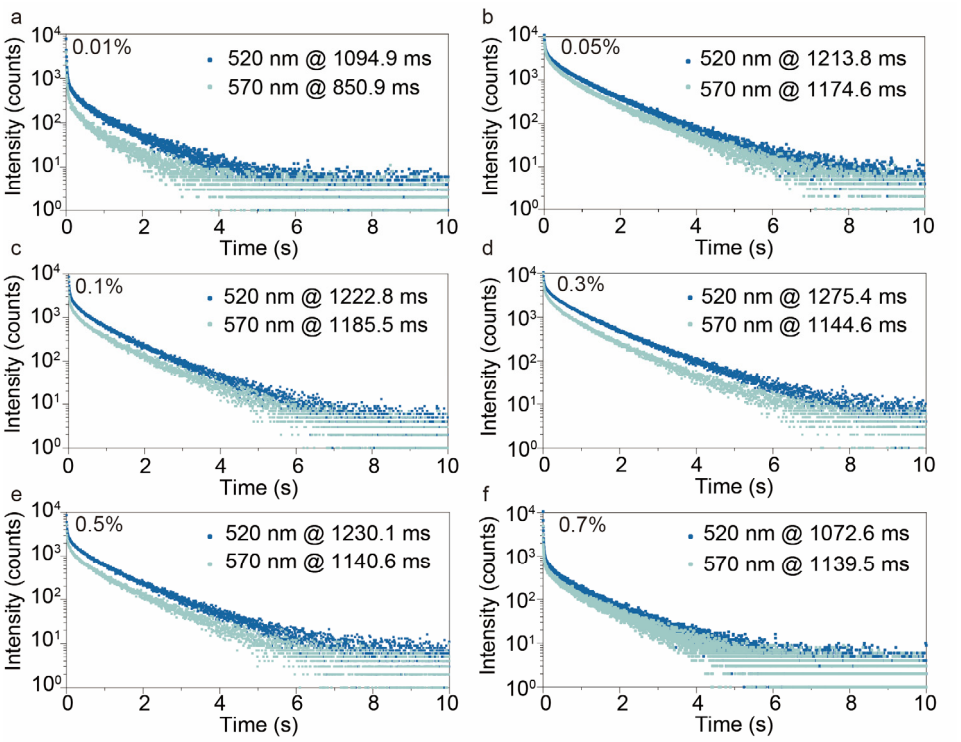

Fig. S34 | Lifetime decay profiles of DBCz@PVM films monitoring emission bands at 520 and 570 nm under ambient conditions. a, 0.01 wt.%. b, 0.05 wt.%. c, 0.1 wt.%. d, 0.3 wt.%. e, 0.5 wt.%. f, 0.7 wt.%.

Table S2 PLQY and Phos. efficiency of DBCz@PVM films at various doping concentrations.

Ratio (%)	Φ_{PL} (%)	$\Phi_{Phos.}$ (%)
0.01	6.3	0.39
0.05	7.4	0.34
0.1	19.9	1.11
0.3	22.5	1.25
0.5	21.3	0.47
0.7	17.6	0.59

Table S3 Phosphorescence lifetime of DBCz@PVM films

Ratio (%)	Wavelength (nm)	Phosphorescence					
		τ_1 (ms)	A_1 (%)	τ_2 (ms)	A_2 (%)	τ_3 (ms)	A_3 (%)
0.01	520	26.0	6.91	255.1	25.05	1094.9	68.04
	570	10.3	21.71	129.6	21.82	850.9	56.47
0.05	520	56.9	3.74	401.7	24.13	1213.8	72.13
	570	56.7	4.87	374.6	29.17	1174.6	65.96
0.1	520	15.0	5.06	510.2	27.61	1222.8	67.33
	570	114.6	7.63	471.3	26.22	1185.5	66.15
0.3	520	99.0	3.73	511.1	26.80	1275.4	69.47
	570	51.2	4.31	366.1	27.84	1144.6	67.84
0.5	520	61.5	4.00	422.3	26.04	1230.1	69.96
	570	24.3	4.60	303.0	26.21	1140.6	69.19
0.7	520	27.2	5.15	301.6	25.51	1072.6	69.34
	570	10.5	8.17	220.1	17.77	1139.5	74.06

Table S4 Dynamic photophysical parameters of DBCz@PVM films at various doping concentrations.

Ratio (%)	Wavelength (nm)	Fluorescence					Phosphorescence			
		τ_{Fluo} (ns)	Φ (%)	K_r^{Fluo} (s^{-1})[a]	K_{nr}^{Fluo} (s^{-1})[b]	K_{isc} (s^{-1})[c]	τ_{Phos} (ms)	Φ (%)	K_r^{Phos} (s^{-1})[d]	K_{nr}^{Phos} (s^{-1})[e]
0.01	395	5.00	6.3	1.26×10^7	1.87×10^8	0.78×10^6				
	520						1094.9	0.39	3.56×10^{-3}	0.91
0.05	395	4.32	7.4	1.71×10^7	2.14×10^8	0.79×10^6				
	520						1213.8	0.34	2.80×10^{-3}	0.82
0.1	395	4.59	19.9	4.34×10^7	1.75×10^8	2.42×10^6				
	520						1222.8	1.11	9.08×10^{-3}	0.81
0.3	395	3.37	22.5	6.68×10^7	2.30×10^8	3.71×10^6				
	520						1275.4	1.25	9.80×10^{-3}	0.77
0.5	395	3.62	21.3	5.88×10^7	2.17×10^8	1.30×10^6				
	520						1230.1	0.47	3.82×10^{-3}	0.81
0.7	395	2.21	17.6	7.96×10^7	3.73×10^8	2.67×10^6				
	520						1072.6	0.59	5.50×10^{-3}	0.93

[a] $k_r^{Fluo.} = \Phi_{Fluo.} / \tau_{Fluo.}$; [b] $k_{nr}^{Fluo.} = (1- \Phi_{Fluo.} - \Phi_{Phos.}) / \tau_{Fluo.}$; [c] $k_{isc} = \Phi_{Phos.} / \tau_{Fluo.}$; [d] $k_r^{Phos.} = \Phi_{Phos.} / \tau_{Phos.}$;

[e] $k_{nr}^{Phos.} = (1- \Phi_{Phos.}) / \tau_{Phos.}$

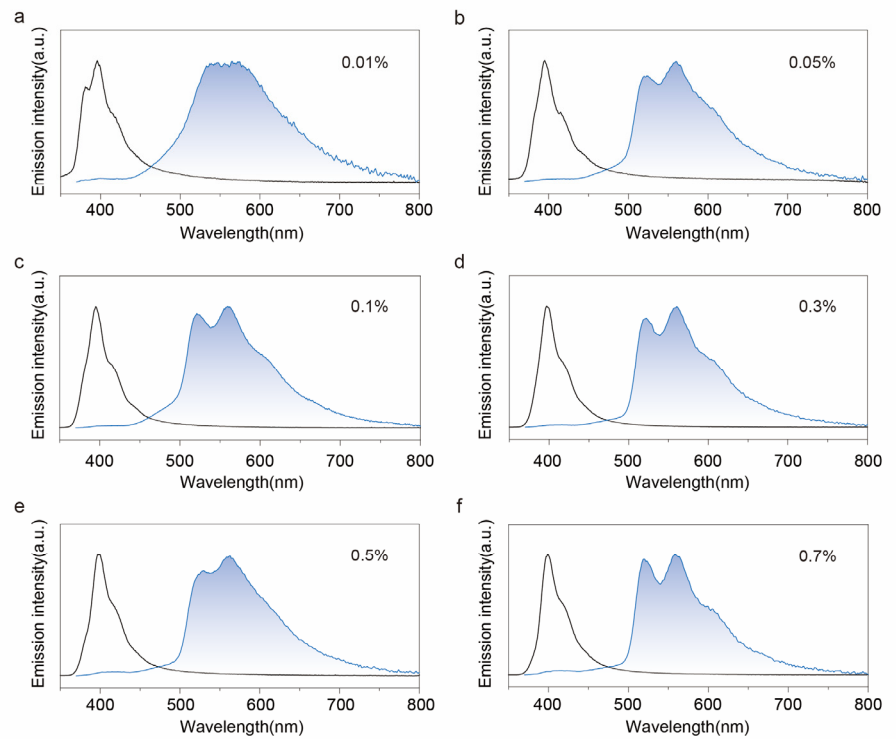

Fig. S35 | Normalized steady-state photoluminescence (black lines) and phosphorescence (blue lines) spectra of DBCz in PBM films**.** a, 0.01 wt.%. b, 0.05 wt.%. c, 0.1 wt.%. d, 0.3 wt.%. e, 0.5 wt.%. f, 0.7 wt.%.

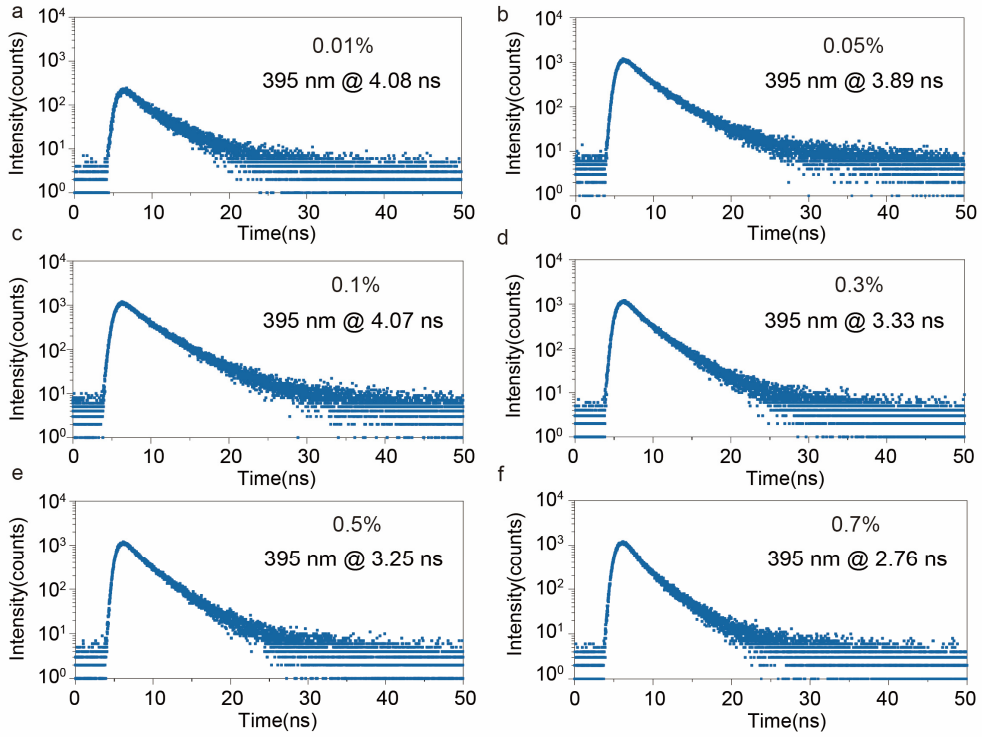

Fig. S36 | Fluorescence lifetime of DBCz@PBM films under ambient conditions. a, 0.01 wt.%. b, 0.05 wt.%. c, 0.1 wt.%. d, 0.3 wt.%. e, 0.5 wt.%. f, 0.7 wt.%.

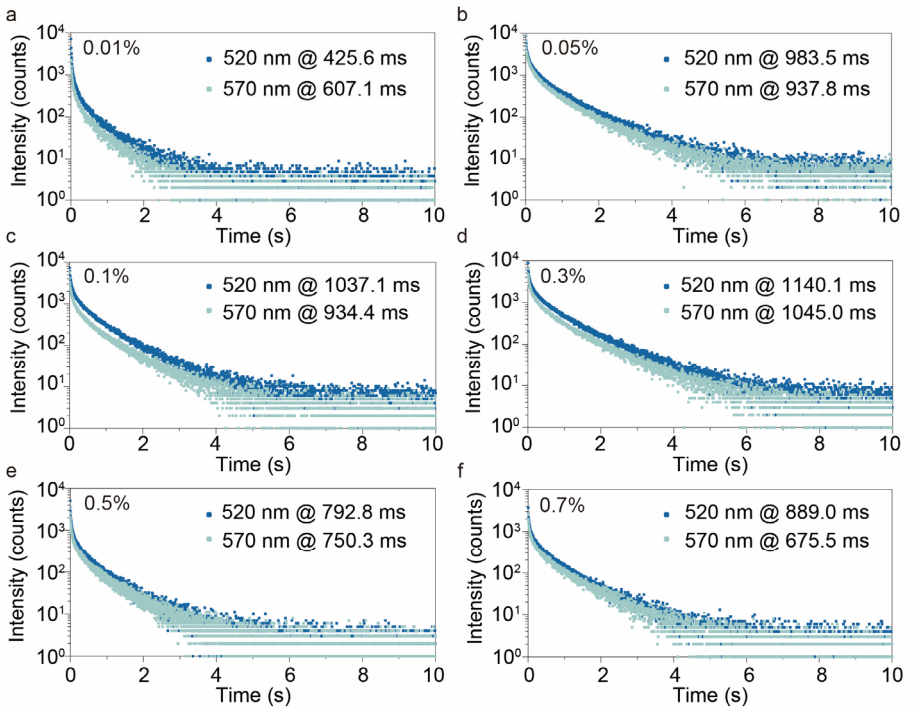

Fig. S37 | Lifetime decay profiles of DBCz@PBM films monitoring emission bands at 520 and 570 nm under ambient conditions. a, 0.01 wt.%. b, 0.05 wt.%. c, 0.1 wt.%. d, 0.3 wt.%. e, 0.5 wt.%. f, 0.7 wt.%.

Table S5 Phosphorescence lifetime of DBCz@PBM films

Ratio (%)	Wavelength (nm)	Phosphorescence					
		τ_1 (ms)	A_1 (%)	τ_2 (ms)	A_2 (%)	τ_3 (ms)	A_3 (%)
0.01	520	11.8	15.58	73.3	31.68	425.6	52.73
	570	10.7	20.36	103.2	32.81	607.1	46.83
0.05	520	31.3	6.27	238. 9	25.3	983.5	68.5
	570	26.1	7.44	213.8	30.51	937.8	62.05
0.1	520	114.8	6.76	427.8	37.13	1037.1	56.1
	570	77.23	5.21	311.7	30.19	934.4	64.60
0.3	520	85.3	7.62	414.9	32.31	1140.1	60.07
	570	65.6	7.05	326.2	29.44	1045.0	63.52
0.5	520	45.9	6.77	227.6	33.92	792.8	59.31
	570	37.6	8.39	175.8	32.26	750.3	59.35
0.7	520	16.7	8.77	185.3	28.17	889.0	63.06
	570	11.4	10.48	119.1	32.00	675.5	57.51

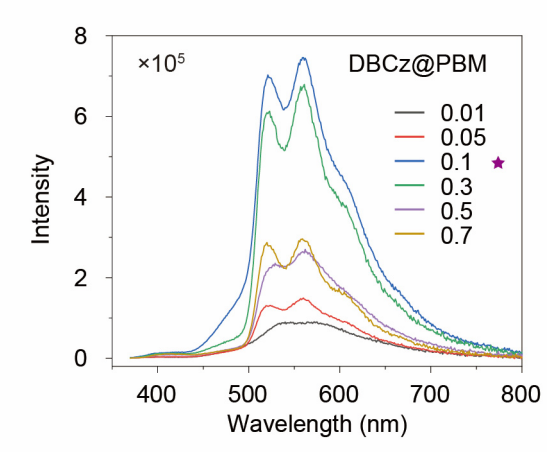

Fig. S38 | Phosphorescence intensity of DBCz doped in PBM films with different doping concentrations at room temperature.

Table S6 PLQY and Phos. efficiency of DBCz@PBM films at various doping concentrations.

Ratio (%)	Φ_{PL} (%)	$\Phi_{Phos.}$ (%)
0.01	5.0	0.36
0.05	10.6	0.59
0.1	18.1	1.1
0.3	18.4	0.76
0.5	11.5	0.69
0.7	13.0	0.66

Table S7 Dynamic photophysical parameters of DBCz@PBM films at various doping concentrations.

Ratio (%)	Wavelength (nm)	Fluorescence					Phosphorescence			
		τ_{Fluo} (ns)	Φ (%)	K_r^{Fluo} (s^{-1})[a]	K_{nr}^{Fluo} (s^{-1})[b]	K_{isc} (s^{-1})[c]	τ_{Phos} (ms)	Φ (%)	K_r^{Phos} (s^{-1})[d]	K_{nr}^{Phos} (s^{-1})[e]
0.01	395	4.08	5.0	1.23×10^{7}	2.33×10^{8}	0.88×10^{6}				
	520						425.6	0.36	8.46×10^{-3}	2.34
0.05	395	3.89	10.6	2.72×10^{7}	2.30×10^{8}	1.52×10^{6}				
	520						983.5	0.59	6.00×10^{-3}	1.01
0.1	395	4.07	18.1	4.45×10^{7}	2.01×10^{8}	2.70×10^{6}				
	520						1037.1	1.1	10.6×10^{-3}	0.95
0.3	395	3.33	18.4	5.53×10^{7}	2.45×10^{8}	2.28×10^{6}				
	520						1140.1	0.76	6.67×10^{-3}	0.87
0.5	395	3.25	11.5	3.54×10^{7}	2.72×10^{8}	2.12×10^{6}				
	520						792.8	0.69	8.70×10^{-3}	1.25
0.7	395	2.76	13.0	4.71×10^{7}	3.15×10^{8}	2.39×10^{6}				
	520						889.0	0.66	7.42×10^{-3}	1.12

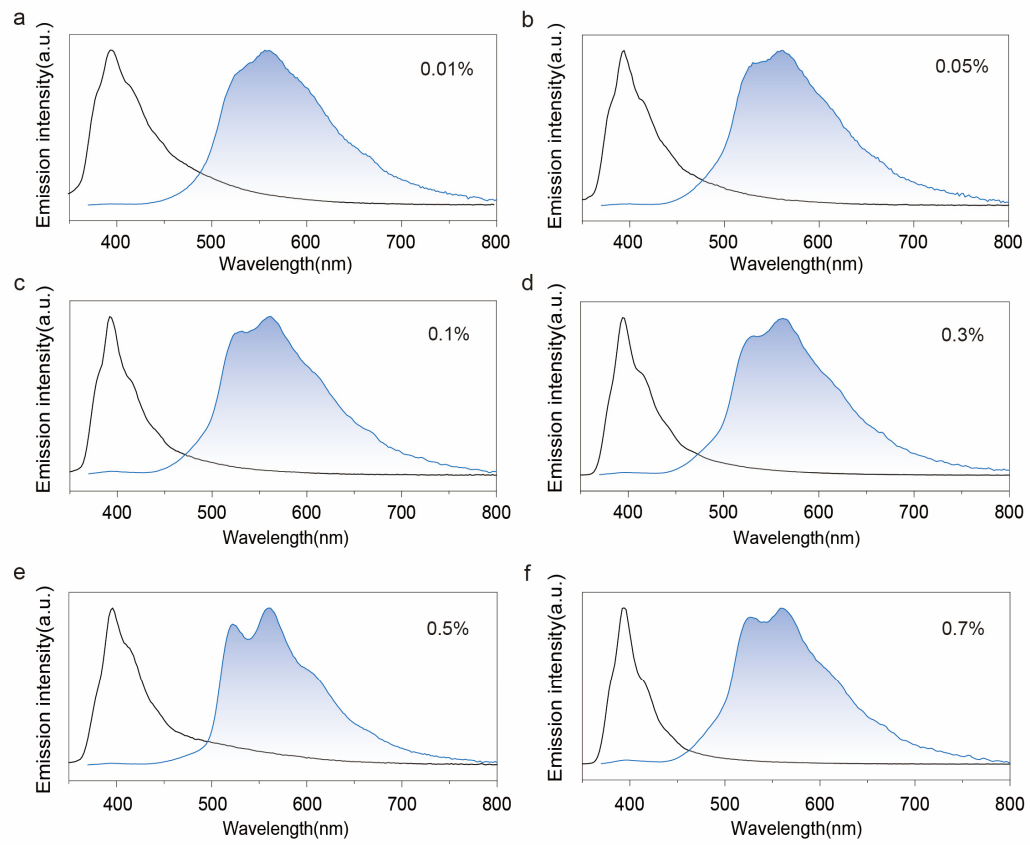

Fig. S39 | Normalized steady-state photoluminescence (black lines) and phosphorescence (blue lines) spectra of DBCz in PSM films. a, 0.01 wt.%. b, 0.05 wt.%. c, 0.1 wt.%. d, 0.3 wt.%. e, 0.5wt.%. f, 0.7 wt.%.

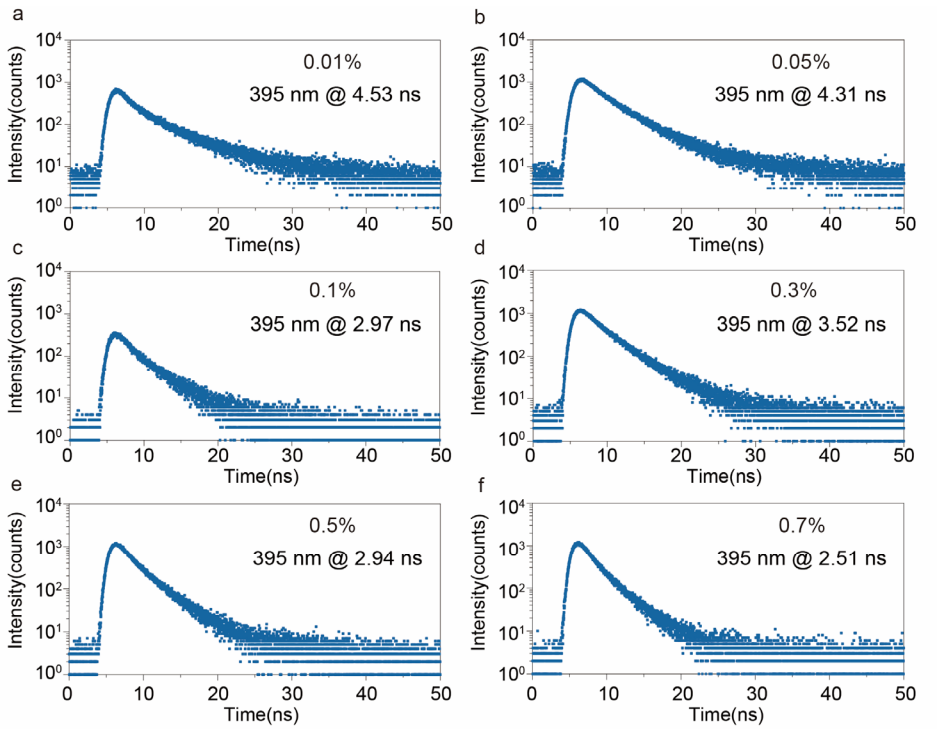

Fig. S40 | Fluorescence lifetime of DBCz@PSM films under ambient conditions. a, 0.01 wt.%. b, 0.05 wt.%. c, 0.1 wt.%. d, 0.3 wt.%. e, 0.5 wt.%. f, 0.7 wt.%.

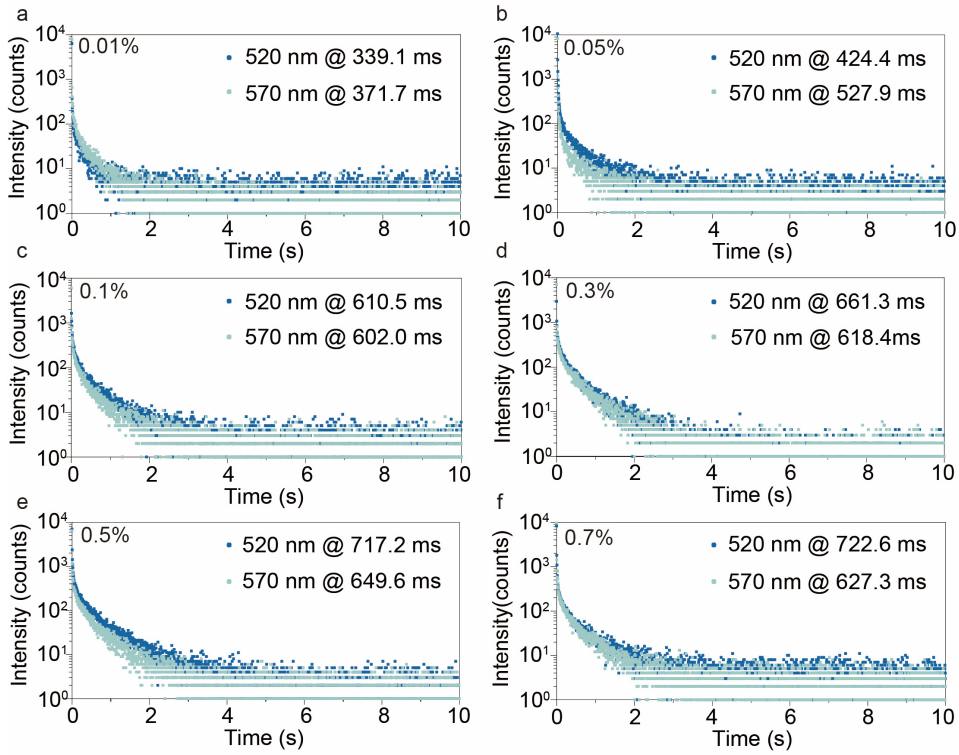

Fig. S41 | Lifetime decay profiles of DBCz@PSM films monitoring emission bands at 520 and 570 nm under ambient conditions. a, 0.01 wt.%. b, 0.05 wt.%. c, 0.1 wt.%. d, 0.3 wt.%. e, 0.5 wt.%. f, 0.7 wt.%.

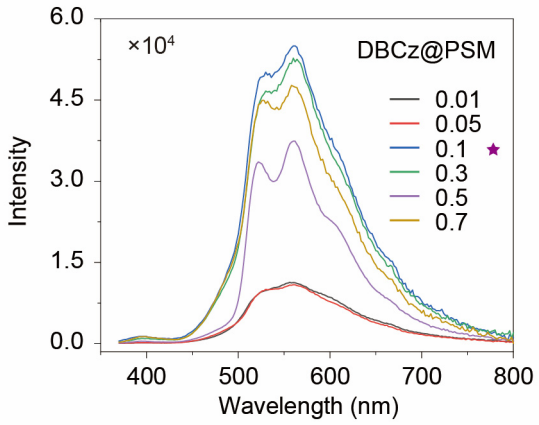

Fig. S42 | Phosphorescence intensity of DBCz doped in PSM films with different doping concentrations at room temperature.

Table S8 Phosphorescence lifetime of DBCz@PSM films

Ratio (%)	Wavelength (nm)	Phosphorescence					
		τ_1 (ms)	A_1 (%)	τ_2 (ms)	A_2 (%)	τ_3 (ms)	A_3 (%)
0.01	520	7.4	32.15	66.8	41.40	339.1	26.45
	570	14.1	13.94	92.5	49.58	371.7	36.48
0.05	520	8.7	33.71	76.5	31.30	424.4	34.98
	570	26.2	16.04	158.2	50.53	527.9	33.43
0.1	520	11.1	18.07	100.2	29.59	610.5	52.34
	570	18.4	17.37	147.4	37.77	602.0	44.86
0.3	520	63.5	9.35	216.3	24.42	661.3	66.23
	570	16.7	9.34	158.8	32.77	618.4	57.89
0.5	520	11.1	14.70	144.4	28.63	717.2	56.67
	570	20.8	8.27	180.2	35.51	649.6	56.23
0.7	520	15.4	5.63	148.7	32.20	722.6	62.17
	570	9.5	16.52	122.8	29.19	627.3	54.29

Table S9 PLQY and Phos. efficiency of DBCz@PSM films at various doping concentrations.

Ratio (%)	Φ_{PL} (%)	$\Phi_{Phos.}$ (%)
0.01	4.6	0.38
0.05	7.1	0.49
0.1	10.6	0.84
0.3	11.8	0.96
0.5	11.7	1.47
0.7	11.0	0.69

Table S10 Dynamic photophysical parameters of DBCz@PSM films at various doping concentrations.

Ratio (%)	Wavelength (nm)	Fluorescence					Phosphorescence			
		τ_{Fluo} (ns)	Φ (%)	K_r^{Fluo} (s^{-1})[a]	K_{nr}^{Fluo} (s^{-1})[b]	K_{isc} (s^{-1})[c]	τ_{Phos} (ms)	Φ (%)	K_r^{Phos} (s^{-1})[d]	K_{nr}^{Phos} (s^{-1})[e]
0.01	395	4.53	4.6	1.02×10^{7}	2.11×10^{8}	0.84×10^{6}				
	520						339.1	0.38	11.2×10^{-3}	2.94
0.05	395	4.31	7.1	1.65×10^{7}	2.16×10^{8}	1.14×10^{6}				
	520						424.4	0.49	11.5×10^{-3}	2.34
0.1	395	2.97	10.6	3.57×10^{7}	3.01×10^{8}	2.83×10^{6}				
	520						610.5	0.84	13.8×10^{-3}	1.62
0.3	395	3.52	11.8	3.35×10^{7}	2.51×10^{8}	2.73×10^{6}				
	520						661.3	0.96	14.5×10^{-3}	1.50
0.5	395	2.94	11.7	3.98×10^{7}	3.00×10^{8}	5.00×10^{6}				
	520						717.2	1.47	20.5×10^{-3}	1.37
0.7	395	2.51	11.0	4.38×10^{7}	3.55×10^{8}	2.75×10^{6}				
	520						722.6	0.69	9.55×10^{-3}	1.37

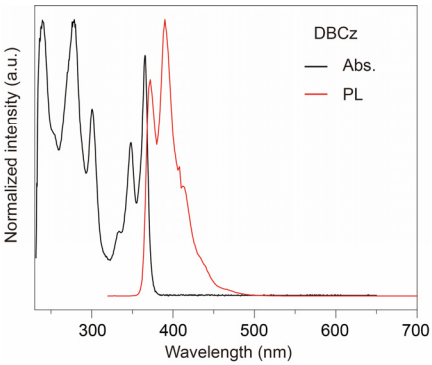

Fig. S43 | Normalized absorption (Abs, black line) and steady-state photoluminescence (PL, red line) spectra of DBCz in DCM solution (1 x 10^{-5} M) at room temperature, respectively.

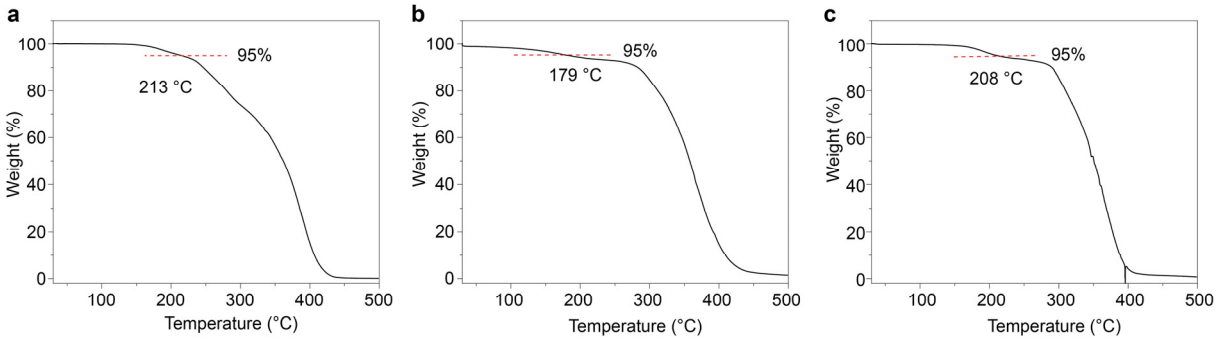

Fig. S44 | TGA curves of a) PBM, b) PVM, and c) PSM films.

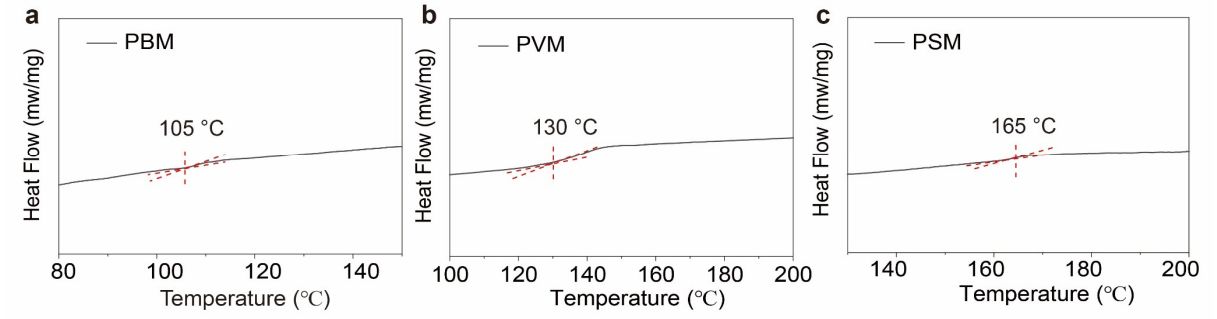

Fig. S45 | DSC curves of a) PBM, b) PVM, and c) PSM films.

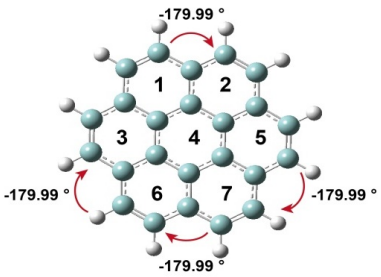

Fig. S46 | Chemical structure of the Cone molecule.

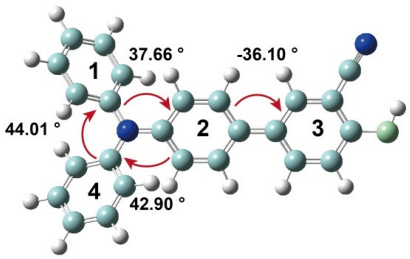

Fig. S47 | Chemical structure of the TPCN molecule.

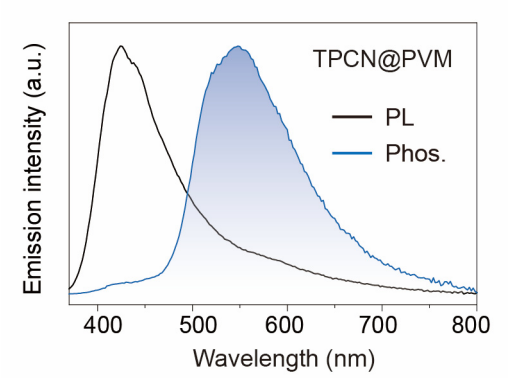

Fig. S48 | Steady-state photoluminescence (black line) and phosphorescence (blue line) spectra of TPCN@PVM at 77 K.

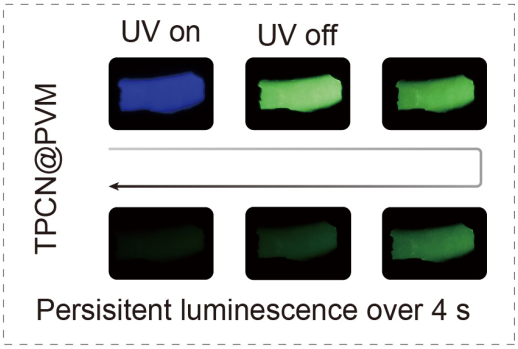

Fig. S49 | Photographs of TPCN@PVM films taken under a 365 nm lamp on and off.

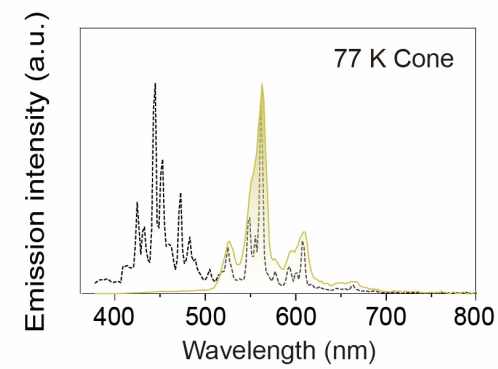

Fig. S50 | Steady-state photoluminescence (black line) and phosphorescence (yellow line) spectra of Cone in dilute *m*-THF solution (1×10^{-5} M) at 77 K.

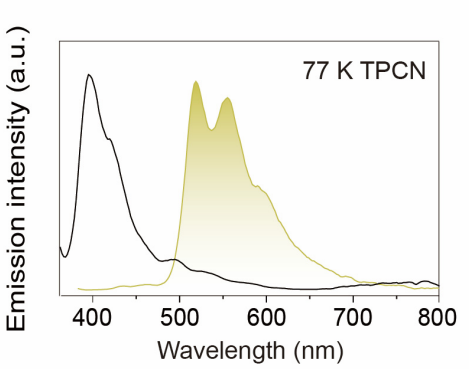

Fig. S51 | Steady-state photoluminescence (black line) and phosphorescence (yellow line) spectra of TPCN in dilute *m*-THF solution (1×10^{-5} M) at 77 K.

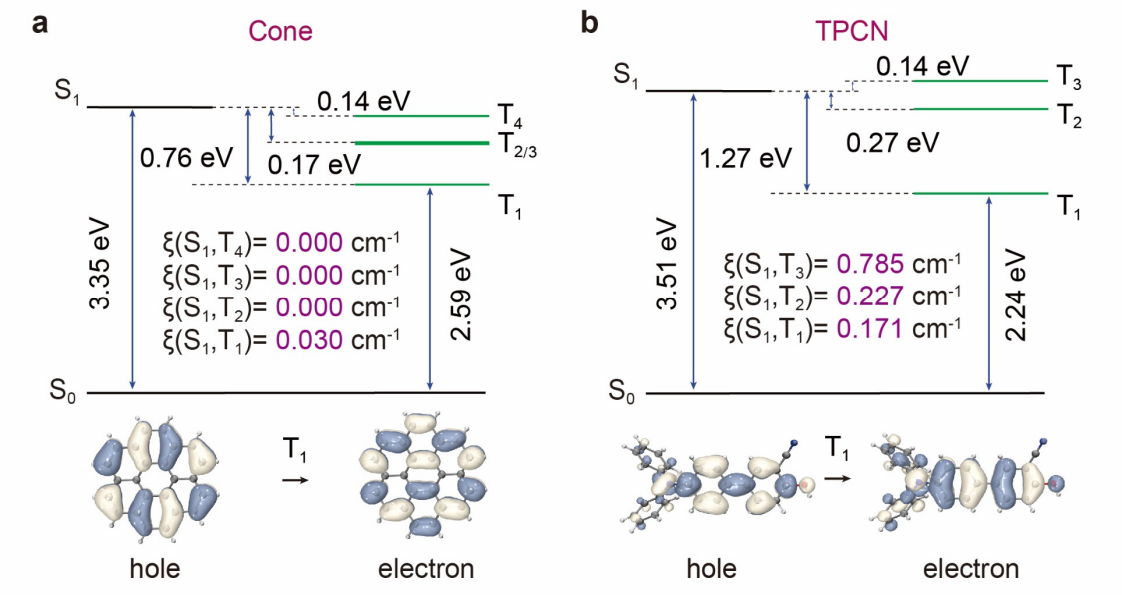

Fig. S52 Natural transition orbitals (NTO), energy diagram, and spin-orbital coupling (ξ) of a) Cone and b) TPCN.

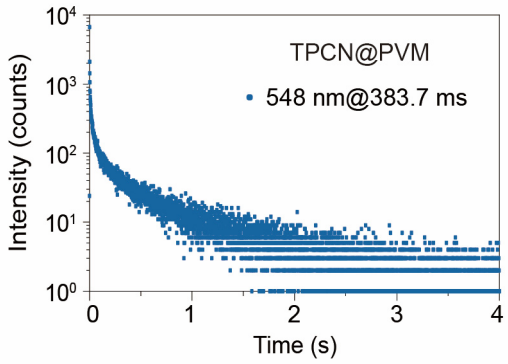

Fig. S53 | Lifetime decay profiles of TPCN@PVM films monitoring emission band at 548 nm under ambient conditions.

Table S11 PLQY and Phos. efficiency of Cone@PVM and TPCN@PVM films.

Compound	Φ_{PL} (%)	$\Phi_{Phos.}$ (%)
Cone@PVM	19.6	1.02
Cone@PSM	19.5	1.09
TPCN@PVM	44.3	11.38
TPCN@PSM	42.4	6.05

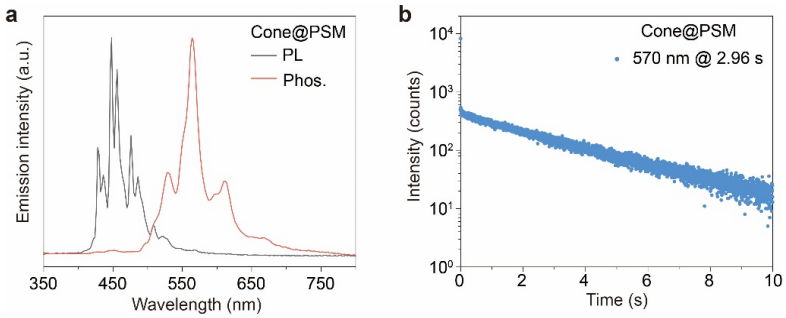

Fig. S54 | (a) Normalized steady-state photoluminescence (black line) and phosphorescence spectra (green line) of Cone@PSM film under ambient conditions. (b) Lifetime decay curve of Cone@PSM films at 570 nm under ambient conditions.

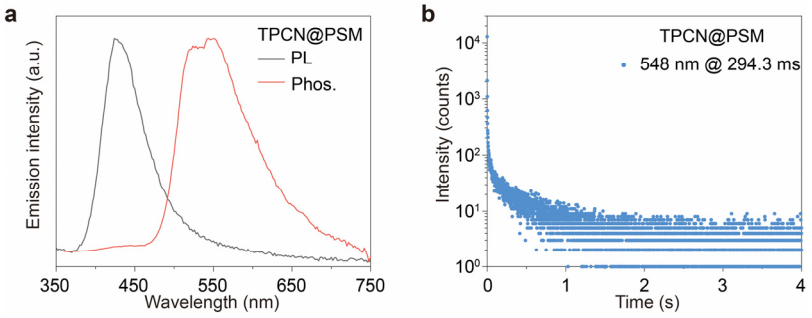

Fig. S55 | (a) Normalized steady-state photoluminescence (black line) and phosphorescence spectra (green line) of TPCN@PSM film under ambient conditions. (b) Lifetime decay curve of TPCN@PSM films at 548 nm under ambient conditions.

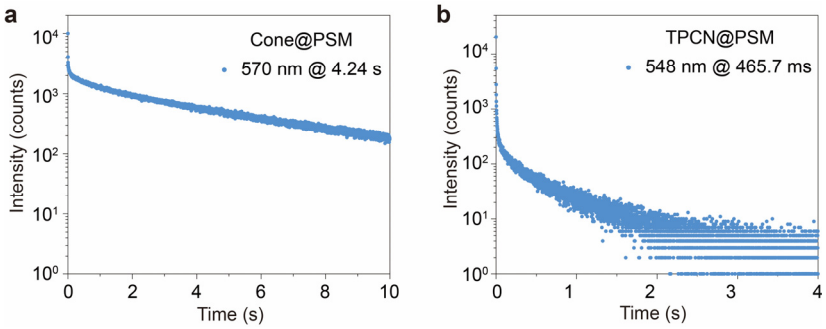

Fig. S56 | Phosphorescence lifetime of Cone@PSM and TPCN@PSM under vacuum conditions at room temperature.

Supplementary References

1. M. Petersilka, U. J. Gossmann, E. K. U. Gross, *Phys. Rev. Lett*. **1996**, *76*, 1212.
2. M. Frisch, et al. Gaussian 09, Revision C.01. Gaussian, Inc., Wallingford CT, **2009**.
3. F. Neese, Wiley Interdiscip. *Rev.: Comput. Mol. Sci.* **2008**, *8*, e13271.